CHAPTER 5

INFRARED STUDIES OF MG30 COMPLEXES

5.1 Introduction

Fourier transform infrared spectroscopy (FTIR) can be employed to investigate the intermolecular interactions that occur between polymer and salt and between polymer and plasticizer. IR spectra provide information through the wavenumber, intensity, bandwidth and shift of the bands. Many researchers [Wang *et al.*, 2011; Mahmoudian *et al.*, 2011; Ramesh *et al.*, 2011; Majid and Arof, 2008; Winie and Arof, 2006; Deepa *et al.*, 2004] have used FTIR for investigating polymer electrolyte systems.

Li^+ ions tend to coordinate to the oxygen (O) atoms located at the carbonyl (C=O) and methoxy (O–CH_3) groups of PMMA since the negatively charged O atoms can donate electrons to the cations to form dative bonds. Ali *et al.* (2006) and Kumutha *et al.* (2005) have shown that the most important band to show complexation of MG30 with metal ion from salt is the shifting of the ester group on PMMA which is grafted onto the natural rubber backbone. The shift of the carbonyl (C=O) band to lower wavenumber is proof of complexation.

5.2 Vibrational studies of MG30–$LiCF_3SO_3$ films

In order to investigate changes in IR bands upon the addition of $LiCF_3SO_3$ into MG30, the IR bands of individual MG30 and $LiCF_3SO_3$ have to be known in order to observe the changes of position, intensity and shape of each existing band. Figure 5.1

represents the IR spectrum and vibrational bands for pure MG30 in the region between 2000 and 650 cm^{-1}.

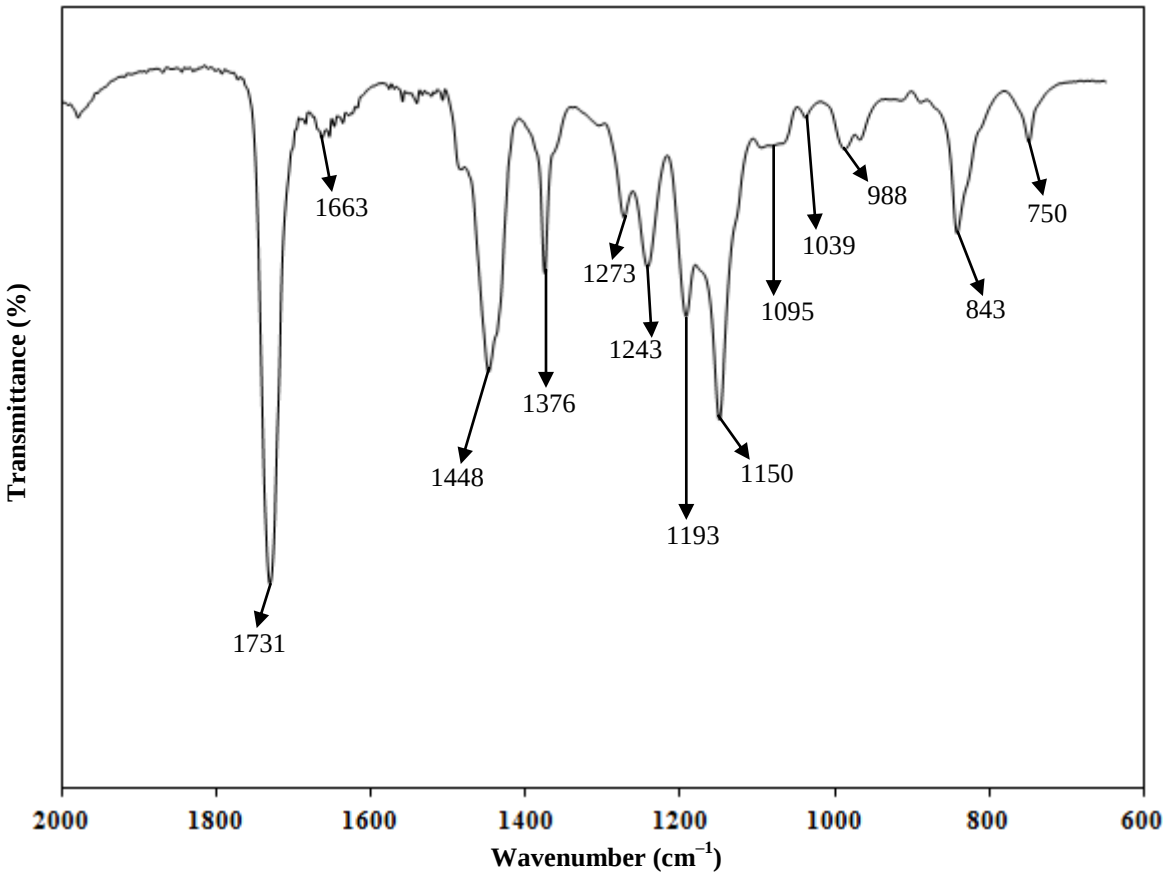

Figure 5.1 FTIR spectrum of MG0L sample

The characteristic peaks observed in pure MG30 are attributed to the functional groups present in natural rubber and PMMA, which are listed in Table 5.1.

Table 5.1: Vibrational assignments of pure MG30

Wavenumber (cm^{-1})	Assignment
1731	ν(C=O) stretching of PMMA
1663	ν(C=C) stretching of polyisoprene
1448	γ(O–CH_3) asymmetric deformation of PMMA
1376	β(CH_3) symmetric deformation of polyisoprene

Table 5.1, continued

1273	ν(C–O) stretching of –COO– of PMMA
1243	$\tau(CH_2)$ twisting mode of polyisoprene
1193	$\delta_s(C–H_2)$ in–plane bending of polyisoprene
1150	$\tau(CH_2)$ twisting mode of PMMA
1095	$\rho(CH_3)$ rocking of polyisoprene
1039	ν(C–C) stretching of polyisoprene
988	ν_s(C–O–C) symmetric stretching of PMMA
843	$C(CH_3)_2$ skeletal vibration of PMMA
750	$\rho(C–H_2)$ rocking of PMMA

Figure 5.2 (a) and (b) depict the FTIR spectrum of $LiCF_3SO_3$ and $LiN(CF_3SO_2)_2$ respectively. The triflate ion is very sensitive to its state of coordination, thus changes to its environment in a mixture can be detected by different infrared vibrations [MacFarlane *et al.*, 1995]. IR vibrational modes of triflate salts have been reported in the literature by Bernson and Lindgren (1995), Subban *et al.* (2004) and Kumar *et al.* (2005). According to Bernson and Lindgren (1995), the asymmetric SO_3 stretch, $\nu_a(SO_3)$ lies in the region between 1340 and 1190 cm^{-1}, the symmetric SO_3 stretch, $\nu_s(SO_3)$ between 1050 to 1000 cm^{-1} and the symmetric CF_3 deformation vibration, $\delta(CF_3)$ from 770 to 750 cm^{-1}.

IR vibrational modes of lithium imide have been reported in the literature by Deepa *et al.* (2000), Deepa *et al.* (2004) and Ahmad *et al.* (2008). Ahmad and coworkers (2008) reported the asymmetric SO_2 stretching mode, $\nu_a(SO_2)$ of lithium imide at 1354 cm^{-1}, the symmetric stretching mode of CF_3, $\nu_s(CF_3)$ at 1192 cm^{-1}, ν_a(S–N–S) mode at 1056 cm^{-1}, combination of ν(C–S) and ν(S–N) modes at ~787 cm^{-1} and ν(S–N) mode at ~739 cm^{-1}. Deepa *et al.* (2004) reported SO_2 stretching modes around

1337–1355 cm^{-1} and 1140 cm^{-1}, ν_a(S–N–S) mode at 1060 cm^{-1} and ν_s(S–N–S) mode at 750 and 739 cm^{-1}. Table 5.2 lists the assignment of bands of $LiCF_3SO_3$ and $LiN(CF_3SO_2)_2$ in this work.

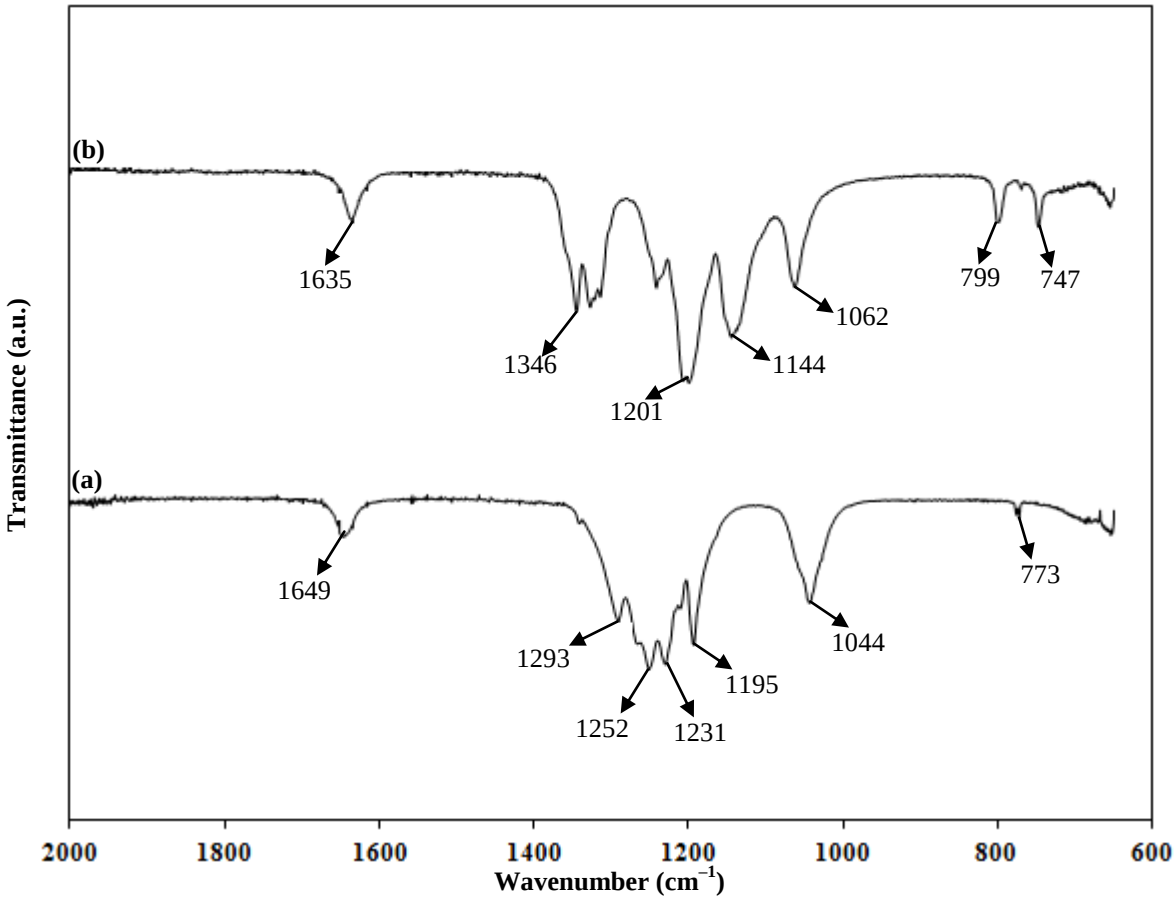

Figure 5.2 FTIR spectra of (a) $LiCF_3SO_3$ and (b) $LiN(CF_3SO_2)_2$

Table 5.2: Vibrational assignments of $LiCF_3SO_3$ and $LiN(CF_3SO_2)_2$

Wavenumber (cm^{-1})		Assignment
$LiCF_3SO_3$	$LiN(CF_3SO_2)_2$	
–	1346	$\nu_a(SO_2)$
1252	–	$\nu_a(SO_3)$
1231	–	$\nu_s(CF_3)$
1195	1201	$\nu_a(CF_3)$
–	1144	$\nu_s(SO_2)$
–	1062	ν_a(S–N–S)
1044	–	$\nu_s(SO_3)$
–	799	ν(C–S) and ν(S–N)
773	–	$\delta(CF_3)$
–	747	ν(S–N)

Figures 5.3 (a) to (i) show the IR spectra of MG30–$LiCF_3SO_3$ polymer electrolyte films in the region from 2000 to 650 cm^{-1}.

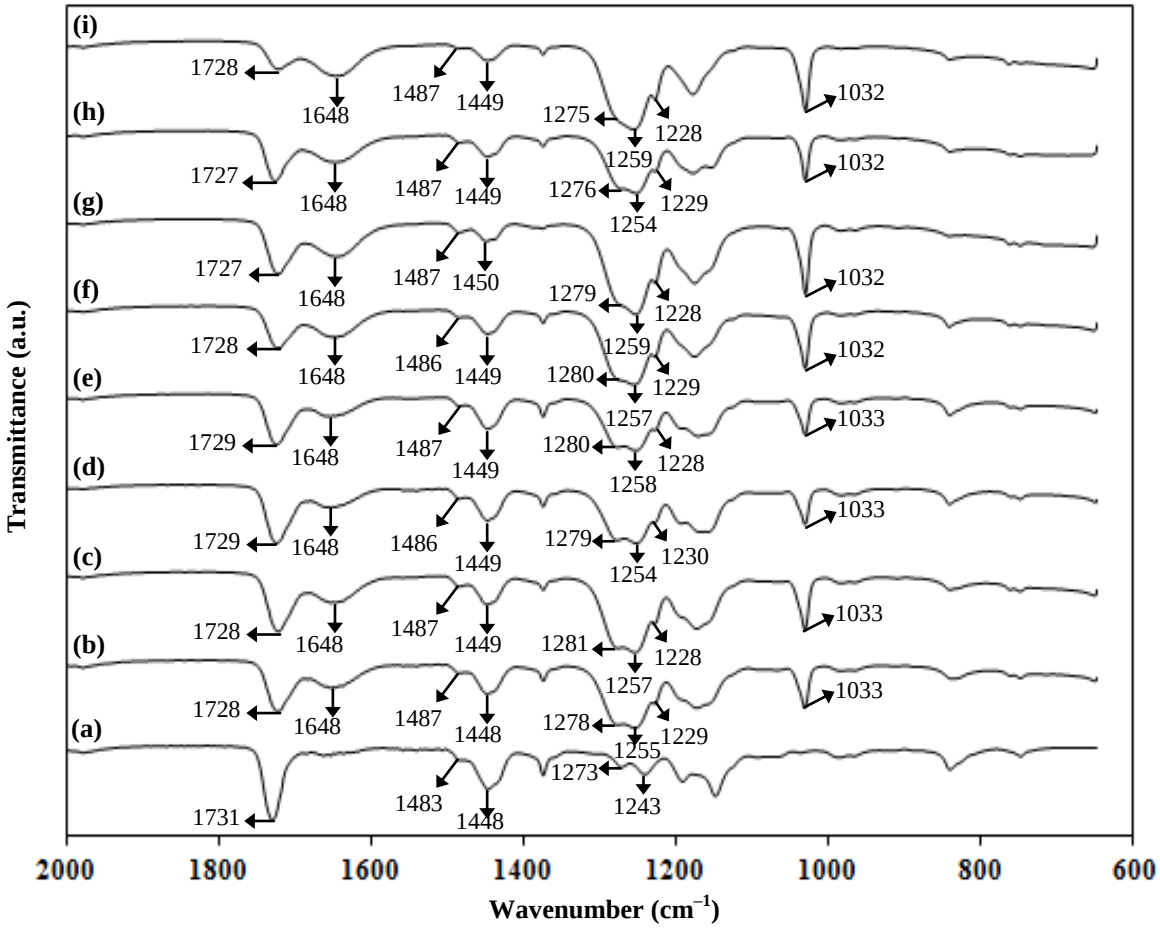

Figure 5.3 FTIR spectra in the region between 2000 and 650 cm^{-1} of (a) MG0L, (b) MG5L, (c) MG10L, (d) MG15L, (e) MG20L, (f) MG25L, (g) MG30L, (h) MG35L and (i) MG40L

The carbonyl (C=O) band in the spectrum of MG30 peaks at 1731 cm^{-1} (Figure 5.4). This is in agreement with the report by Kumutha *et al.* (2004) and Ali *et al.* (2008). As complexation between Li^+ and MG30 can occur at the oxygen atom of the C=O group, changes to the *v*(C=O) band must be investigated.

Upon the incorporation of lithium triflate salt, the *v*(C=O) band is observed to shift from its original position at 1731 cm^{-1} to between 1729 and 1727 cm^{-1} with reduced intensity in the polymer–salt system. This is in agreement with literature

[Deepa *et al.*, 2002a; Deepa *et al.*, 2004] that reported the shifting of the *v*(C=O) band to lower wavenumbers in the polymer–salt complexes. The downshift of *v*(C=O) band is due to weakening of the C=O bond caused by coordination of Li^+ ions at the oxygen atom of C=O group to form C=O——Li^+ bond. Thus, the shift of *v*(C=O) shows that Li^+ ion has coordinated at the oxygen atom of C=O group to form polymer–salt complexes.

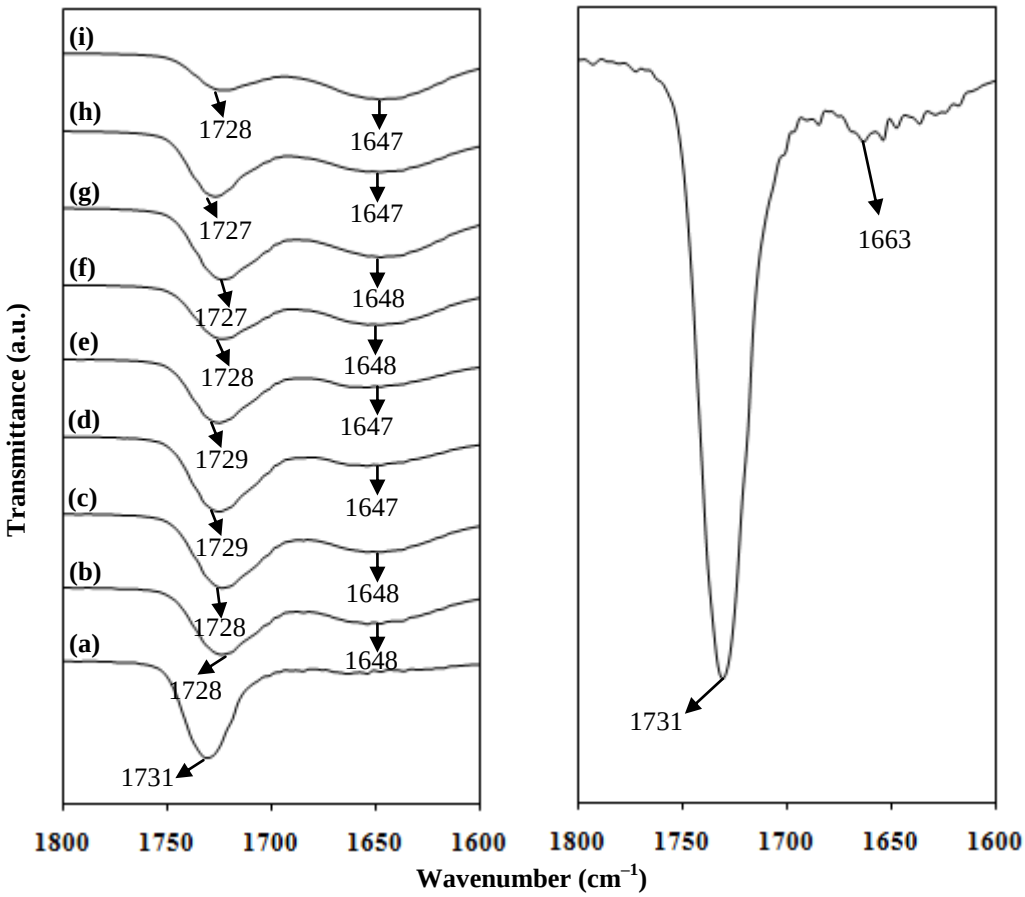

Figure 5.4 FTIR spectra in the region between 1800 and 1600 cm^{-1} of (a) MG0L, (b) MG5L, (c) MG10L, (d) MG15L, (e) MG20L, (f) MG25L, (g) MG30L, (h) MG35L and (i) MG40L. Image on the right is the enlarged IR spectrum of MG0L

In pure MG30 sample, a peak is present at 1663 cm^{-1} as shown in Figure 5.4. According to Ali *et al.* (2008) and Man *et al.* (2008), this peak is assigned to C=C stretching vibration, *v*(C=C) from polyisoprene. The peak has also been detected by other researchers [Alias *et al.*, 2004; Kumutha *et al.*, 2005; Kumutha and Alias, 2006; Ali *et al.*, 2006] in PMMA grafted natural rubber–salt electrolytes. This peak shifts to lower wavenumber on the incorporation of $LiCF_3SO_3$ at ~ 1648 cm^{-1}.

This peak becomes more obvious as more lithium salt was added. This suggests that lithium triflate could have contributed to the growth of this peak. In the spectrum of $LiCF_3SO_3$ shown in Figure 5.2 (a), it can be observed that the salt has a peak at 1649 cm^{-1}. This peak could have overlapped with the *v*(C=C) stretching mode of the polyisoprene to make the band observed at ~ 1648 cm^{-1} more obvious. Kumutha *et al.* (2005) and (2006) also reported the growth of this band between 1645 and 1643 cm^{-1} with increasing lithium salt concentration in MG30–$LiCF_3SO_3$ polymer electrolyte system. The growth of this band in terms of intensity can clearly be observed in the deconvoluted IR bands shown in Figure 5.5.

It can be observed that the band at 1648 cm^{-1} in the spectrum of MG30–$LiCF_3SO_3$ complexes eventually grew in intensity and surpassed the intensity of the C=O bond (1729–1727 cm^{-1}) in the MG30 sample containing 40 wt.% $LiCF_3SO_3$ salt. This indicates that there could be more $LiCF_3SO_3$ salt as compared to available C=O sites for coordination. The FTIR results support the results obtained from SEM and XRD analyses in Chapter 4.

Band envelopes containing several overlapping IR bands in MG10L, MG20L, MG30L and MG40L films between 1520 and 1400 cm^{-1} were deconvoluted as shown in Figure 5.6. Three component bands can be observed in the polymer–salt complexes at 1486–1450 cm^{-1}, 1450–1449 cm^{-1} and 1438–1436 cm^{-1}, which can be attributed to the asymmetric bending of CH bond in –C–CH_3–, –O–CH_3– and CH_2 scissoring vibrational modes of PMMA. These bands were also reported by Deepa *et al.*, (2004) and (2000). Interaction between salt and MG30 also occurred at –O–CH_3– because the band due to this group shifted from 1448 cm^{-1} to between 1449 and 1450 cm^{-1}.

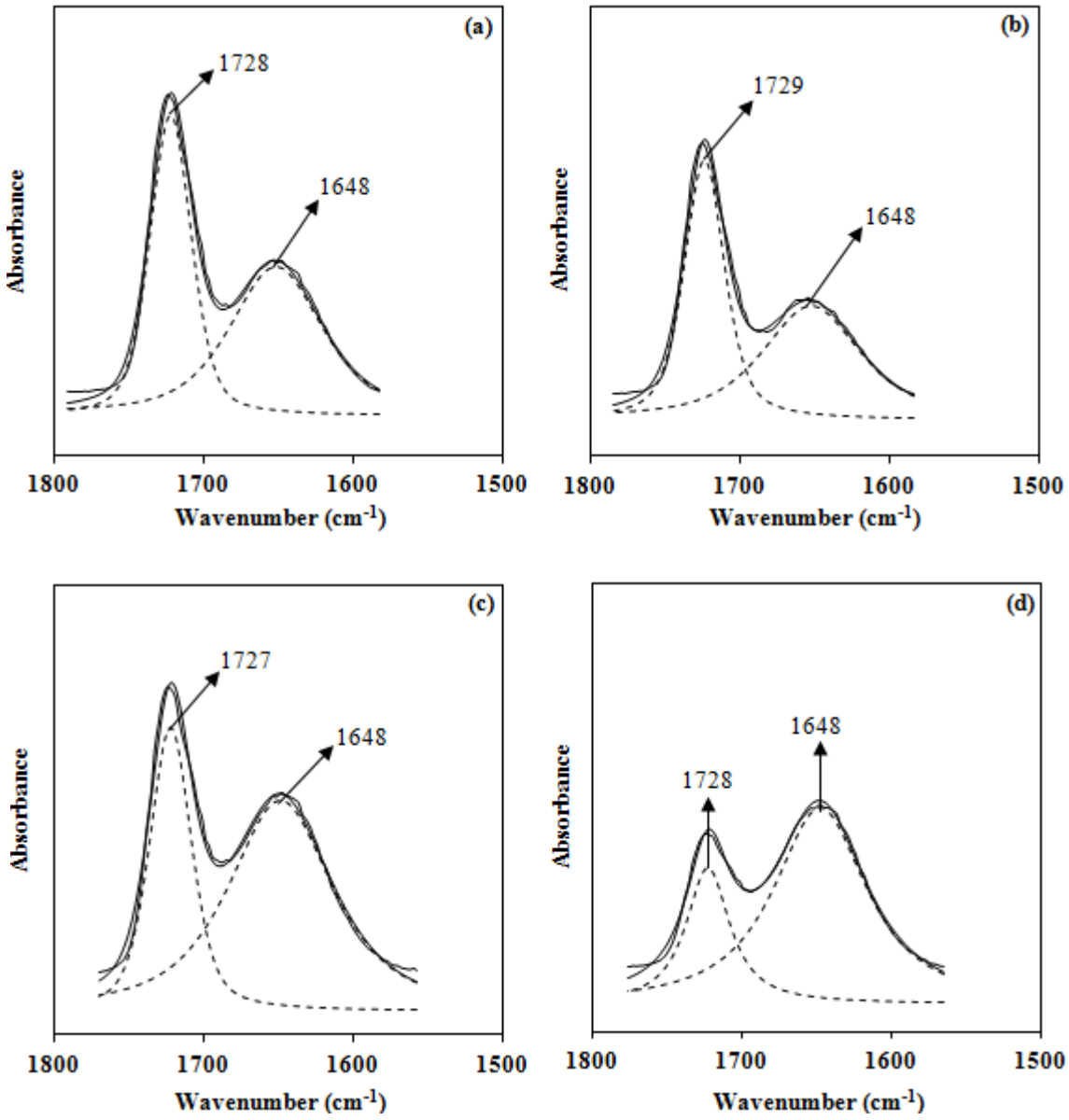

Figure 5.5 Deconvoluted FTIR spectra in the region between 1800 and 1500 cm^{-1} of (a) MG10L, (b) MG20L, (c) MG30L and (d) MG40L

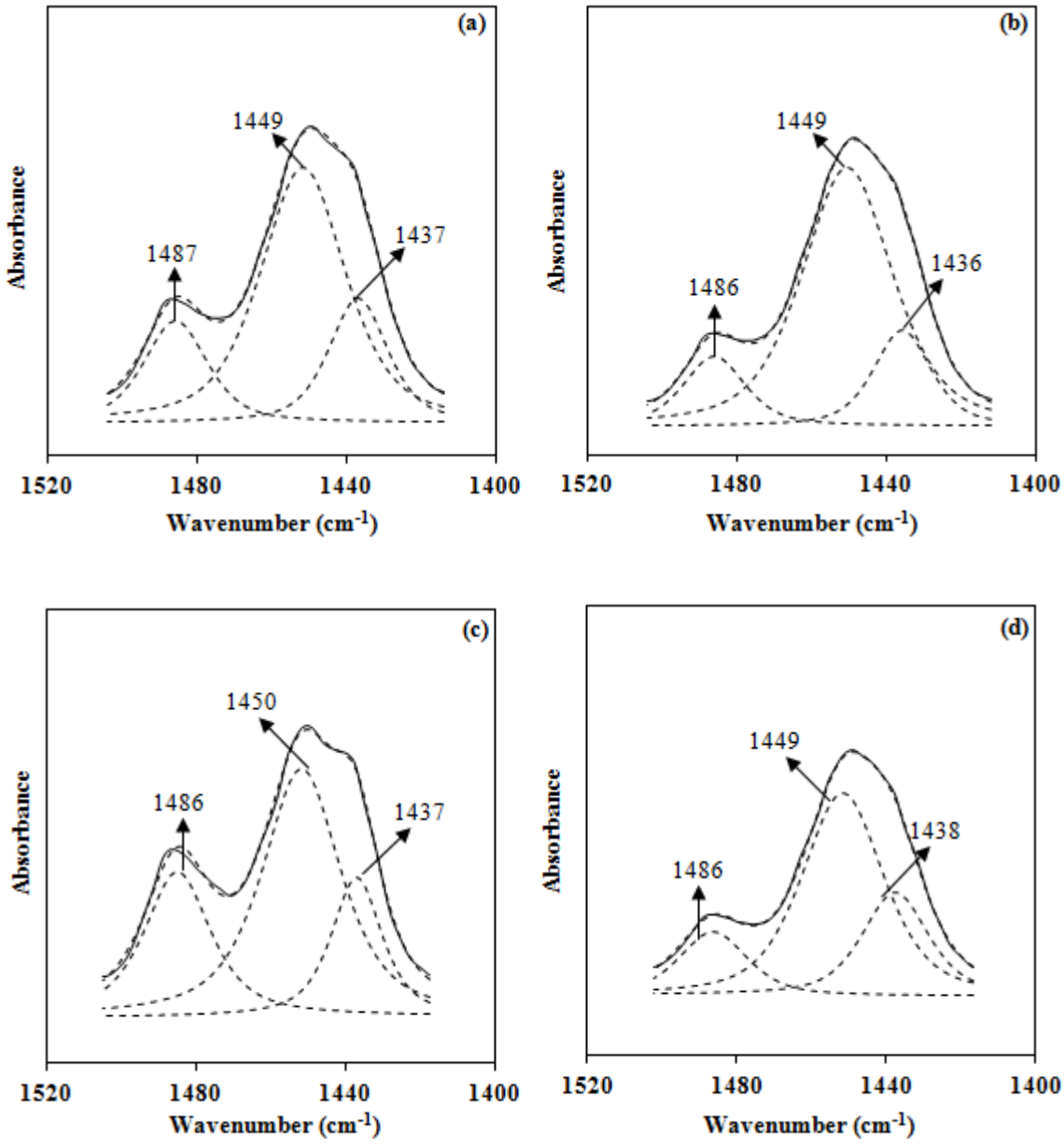

Figure 5.6 Deconvoluted FTIR spectra in the region between 1520 and 1400 cm^{-1} of (a) MG10L, (b) MG20L, (c) MG30L and (d) MG40L

In pure MG30, ν(C–O) of –COO– and $\tau(CH_2)$ twisting modes can be found at 1273 and 1243 cm^{-1}, respectively (Figure 5.7 (a)). Upon the addition of $LiCF_3SO_3$ salt, the two peaks overlapped with three peaks at 1278, 1255 and 1229 cm^{-1} attributed to the lithium triflate salt as can be observed in the IR spectra of the MG30–$LiCF_3SO_3$ samples depicted in Figure 5.7 (a) to (i).

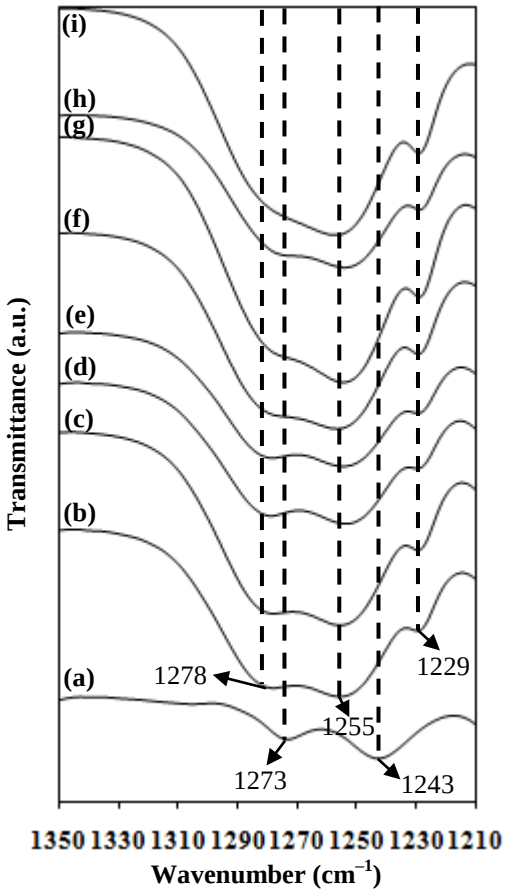

Figure 5.7 FTIR spectra in the region between 1350 and 1210 cm^{-1} of (a) MG0L, (b) MG5L, (c) MG10L, (d) MG15L, (e) MG20L, (f) MG25L, (g) MG30L, (h) MG35L and (i) MG40L

Upon the addition of 5 wt. % $LiCF_3SO_3$, three bands were observed at 1278, 1255 and 1229 cm^{-1}, which are characteristic bands of pure $LiCF_3SO_3$. These bands have shifted from their original positions at 1293 cm^{-1}, 1252 cm^{-1} and 1231 cm^{-1} respectively. The overlapping of the three peaks mentioned before was also reported by Ali *et al.* (2008) who also studied MG30–$LiCF_3SO_3$ polymer electrolyte systems. In order to distinguish the peaks that are present in the spectra of MG30–$LiCF_3SO_3$ samples between 1350 and 1210 cm^{-1}, deconvolution was conducted for the IR bands located within this region for MG10L, MG20L, MG30L and MG40L, which are shown in Figure 5.8.

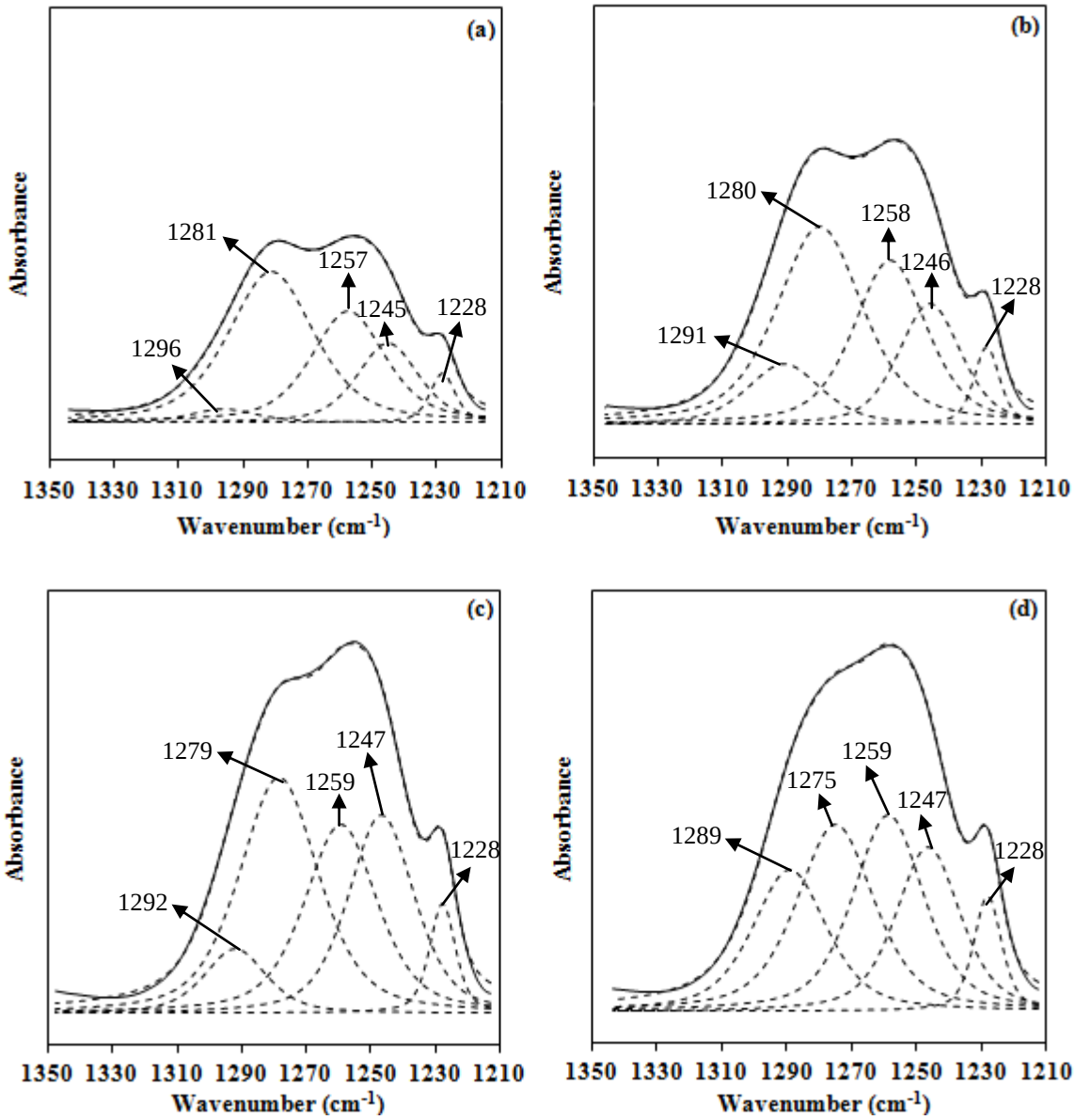

Figure 5.8 Deconvoluted FTIR spectra in the region between 1350 and 1210 cm^{-1} of (a) MG10L, (b) MG20L, (c) MG30L and (d) MG40L

The $LiCF_3SO_3$ band originally located at 1293 cm^{-1} shifted to 1296, 1291, 1292 and 1289 cm^{-1} in MG10L, MG20L, MG30L and MG40L, respectively. The $\nu_a(SO_3)$ band of the salt at 1252 cm^{-1} was also observed to shift to higher wavenumbers between 1257 and 1259 cm^{-1} in the polymer–salt complexes. The $\nu_s(CF_3)$ vibrational mode of $LiCF_3SO_3$ was observed to shift to 1228 cm^{-1} from 1231 cm^{-1} in all the polymer–salt complexes. The shifting of $LiCF_3SO_3$ vibrational modes indicate that the environment around the triflate ion has changed, which could be caused by the coordination of Li^+ ions onto MG30. These $LiCF_3SO_3$ bands also became more intense as the content of

$LiCF_3SO_3$ increased. These shifts indicated interaction has taken place between MG30 and the lithium triflate salt.

The ν(C–O) of –COO– vibrational mode shifted to higher wavenumbers from 1273 to 1279, 1281, 1278 and 1275 cm^{-1} in MG10L, MG20L, MG30L and MG40L samples, respectively. However, the intensity of the ν(C–O) band has reduced from a visible peak to become a shoulder at 1275 cm^{-1} in MG40L sample (Figure 5.9 (d)) implied that coordination of Li^+ on the –C–O– group of MG30 could have decreased. On the other hand, the $\tau(CH_2)$ band belonging to MG30 at 1243 cm^{-1} was observed to shift to higher wavenumbers at 1245 cm^{-1} in MG10L, 1246 cm^{-1} in MG20L and 1247 cm^{-1} in both MG30L and MG40L, respectively. These shifts are evidence of interaction between lithium triflate and the PMMA–grafted natural rubber.

Within the IR region between 1220 and 1100 cm^{-1}, pure MG30 exhibits two vibrational bands at 1193 and 1150 cm^{-1} which are attributed to $\delta_s(CH_2)$ in–plane bending of polyisoprene and $\tau(CH_2)$ twisting of PMMA, as shown in Figure 5.9.

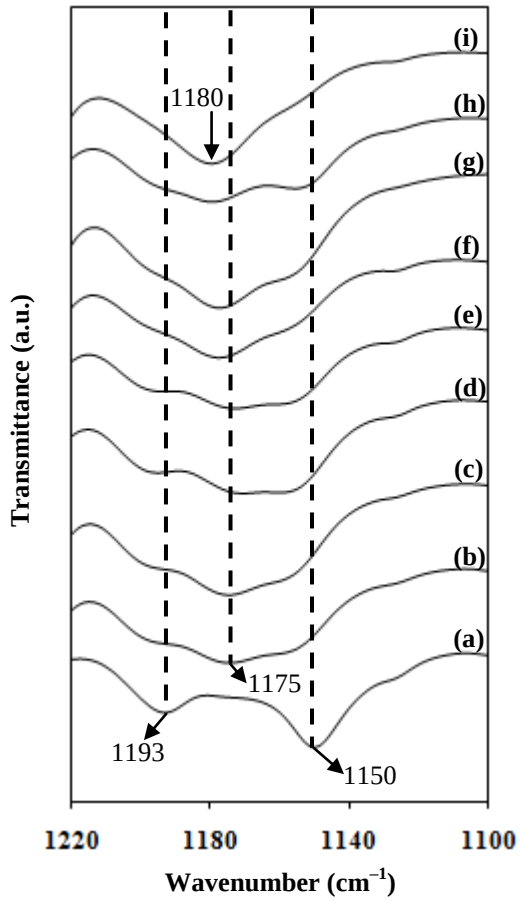

Figure 5.9 FTIR spectra in the region between 1220 and 1100 cm^{-1} of (a) MG0L, (b) MG5L, (c) MG10L, (d) MG15L, (e) MG20L, (f) MG25L, (g) MG30L, (h) MG35L and (i) MG40L

In MG10L and samples containing higher content of lithium salt, changes to the shape of the IR bands in the region between 1220 and 1100 cm^{-1} could clearly be observed. The $\delta_s(CH_2)$ in–plane bending mode originally located at 1193 cm^{-1} is shifted and eventually disappeared in MG40L sample. Another new band located between 1180 and 1173 cm^{-1} could be observed in all the MG30–$LiCF_3SO_3$ samples. This band is attributed to $\nu_a(CF_3)$ mode of pure lithium triflate salt which shifted to lower wavenumbers from its original position at 1195 cm^{-1}. The $\nu_a(CF_3)$ band gradually shifted to higher wavenumbers as the content of salt increased, and was eventually observed at 1180 cm^{-1} in MG40L sample. The band attributed to the $\tau(CH_2)$ twisting of PMMA at 1150 cm^{-1} also shifted to higher wavenumbers in all MG30–$LiCF_3SO_3$ samples. The shifting of the $\delta_s(CH_2)$ in–plane bending of polyisoprene, $\tau(CH_2)$ twisting

of PMMA and $v_a(CF_3)$ stretching modes of lithium triflate salt upon the addition of $LiCF_3SO_3$ salt into MG30 samples has shown that Li^+ ions have coordinated to MG30.

Figure 5.10 shows the $v_s(SO_3)$ mode of pure $LiCF_3SO_3$ located at 1044 cm^{-1}. Upon the addition of lithium triflate into MG30, a new band located around 1033–1032 cm^{-1} could be observed in all MG30–$LiCF_3SO_3$ samples. The downshift of the $v_s(SO_3)$ band is usually observed upon incorporation of $LiCF_3SO_3$ into a polymer host, as reported in PEMA/PVdF–HFP–$LiCF_3SO_3$ [Sim *et al.*, 2011] and PEO–ENR50–$LiCF_3SO_3$ [Noor *et al.*, 2010] polymer electrolyte systems. The shift of $v_s(SO_3)$ mode to lower wavenumbers when incorporated into polymer hosts was also observed by Ali *et al.* (2008).

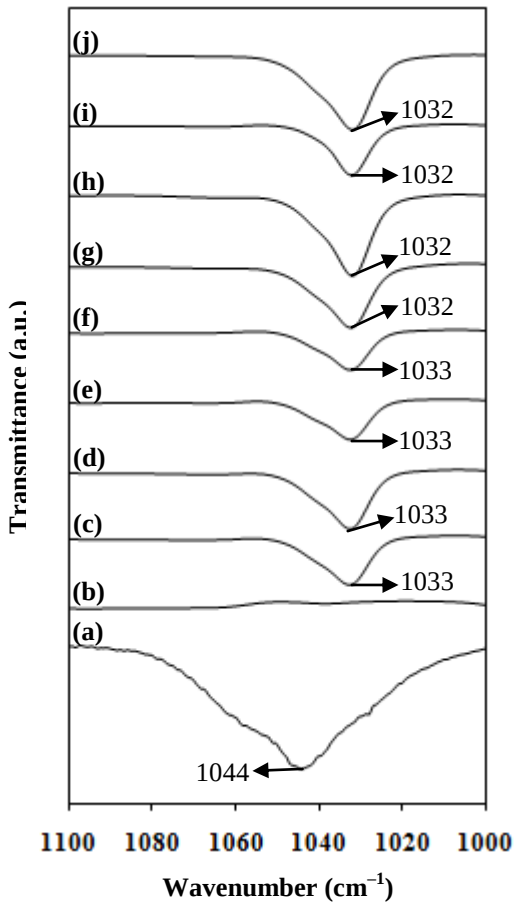

Figure 5.10 FTIR spectra in the region between 1100 and 1000 cm^{-1} of (a) $LiCF_3SO_3$, (b) MG0L, (c) MG5L, (d) MG10L, (e) MG15L, (f) MG20L, (g) MG25L, (h) MG30L, (i) MG35L and (j) MG40L

Huang and Frech (1992) reported that Li^+ cations interact with $CF_3SO_3^-$ anions through the SO_3^- end and that the non–degenerate vibrational mode of $v_s(SO_3)$ can be used to distinguish between free ions (i.e. $CF_3SO_3^-$) at 1034–1030 cm^{-1}, ion–pairs (i.e. $LiCF_3SO_3$, $Li(CF_3SO_3)_2^-$, $Li(CF_3SO_3)_3^{2-}$) at 1045–1040 cm^{-1} and highly–aggregated ions (i.e. $Li_2CF_3SO_3^+$, $Li_3CF_3SO_3^{2+}$) at 1053–1049 cm^{-1}. The fraction of free ions, ion–pairs and ion aggregates have been used by some researchers to correlate with their ionic conductivity results of polymer electrolytes by either Raman or IR spectroscopy [Kim and Oh, 2002; Austin Suthanthiraraj *et al.*, 2010]. In order to distinguish between the different ionic species, deconvolution of the IR bands between 1060 and 1000 cm^{-1} for MG10L, MG20L, MG30L and MG40L samples was carried out and the deconvoluted peaks are shown in Figure 5.11.

Two component peaks attributable to the free ions and ion–pairs of $v_s(SO_3)$ vibrational mode could be detected upon deconvolution of all the polymer–salt complexes. Figure 5.11 (a) to (d) depict the deconvoluted peaks of free ions and ion–pairs of $v_s(SO_3)$ vibrational mode for MG30–$LiCF_3SO_3$ polymer electrolytes. The area of an IR peak is proportional to the relative concentration of the ionic species present in percentage. The peaks of free ions and ion–pairs of $v_s(SO_3)$ vibrational mode were located at 1032 and 1040 cm^{-1} respectively in the polymer–salt complexes regardless of the salt content. In order to observe the fraction of free ions and ion pairs in the samples, area of the peaks corresponding to free ions and ion pairs were plotted against the $LiCF_3SO_3$ salt concentration, as shown in Figure 5.12.

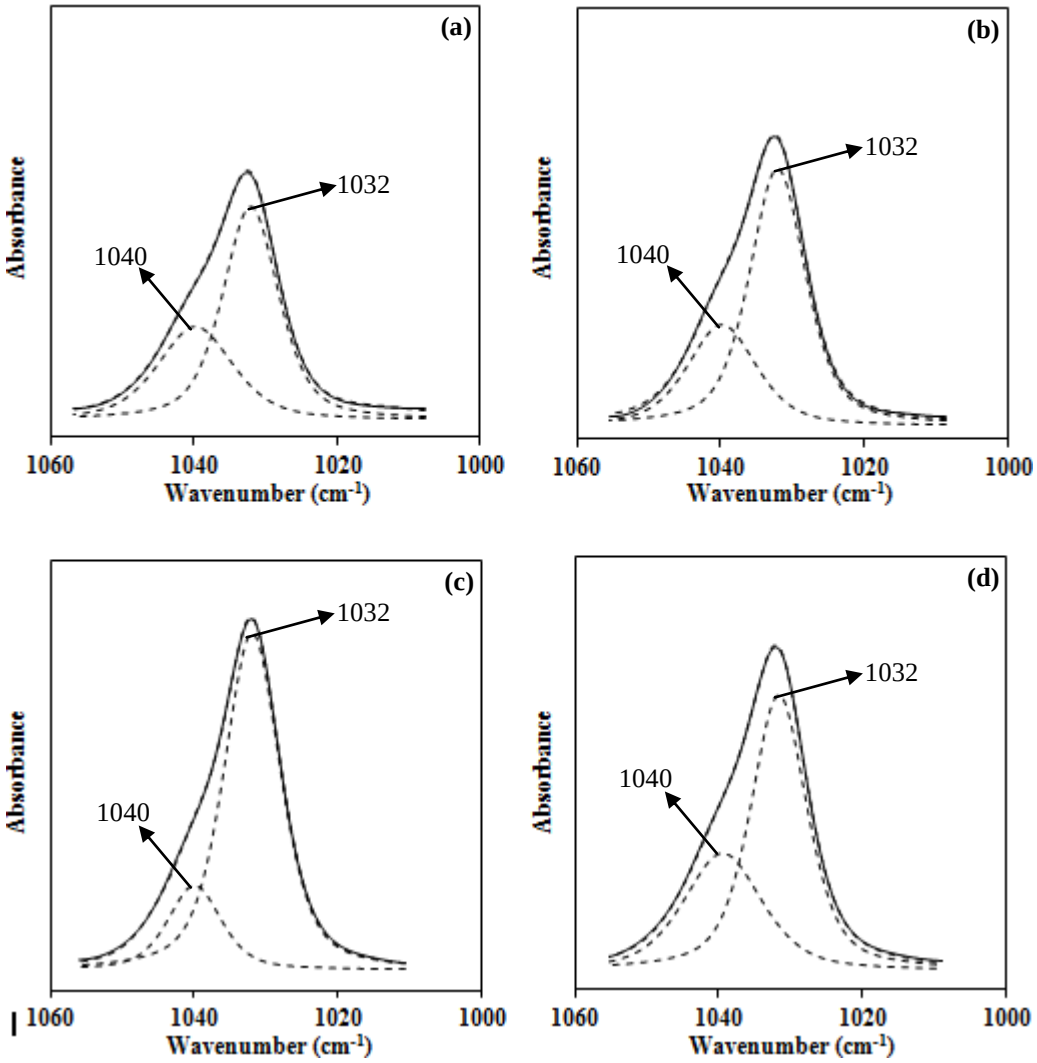

Figure 5.11 Deconvoluted FTIR spectra in the region between 1060 and 1000 cm^{-1} of (a) MG10L, (b) MG20L, (c) MG30L and (d) MG40L

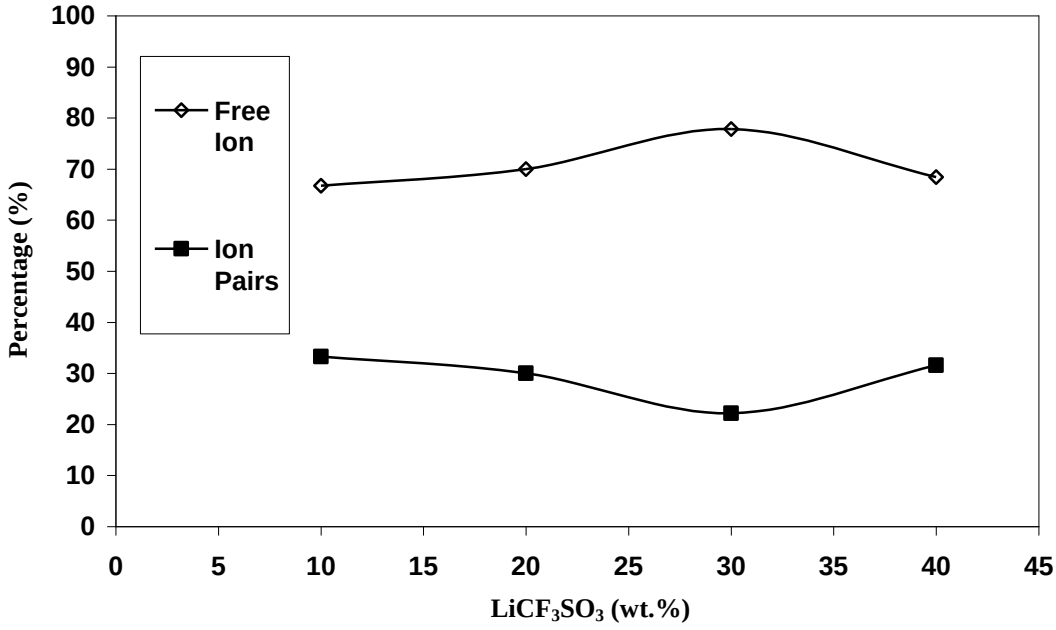

Figure 5.12 Variation of concentration of various states of ions in percentage (%) as a function of $LiCF_3SO_3$

It could be observed that the fraction of free ions and ion pairs increased as the amount of $LiCF_3SO_3$ salt was increased up to 30 wt. %. In all samples, the intensity and area of free triflate ions were found to be noticeably larger than that of ion–pairs. It could be seen that MG30L contained the highest area of the free triflate ions and thus has the highest amount of free Li^+ ions that could contribute to conductivity. These results suggest that MG30L should be the most conducting film in the MG30–$LiCF_3SO_3$ polymer electrolyte system. Other than the $\nu_s(SO_3)$ vibrational mode, Huang and Frech (1992) also found the $\delta(CF_3)$ band usually located in the region from 770 to 750 cm^{-1} to be sensitive to environmental changes around the triflate ion, and thus could be used alongside the $\nu_s(SO_3)$ band in determining the coordination of the triflate salt. Figure 5.13 shows the IR spectra of MG30–$LiCF_3SO_3$ samples between 800 and 700 cm^{-1}.

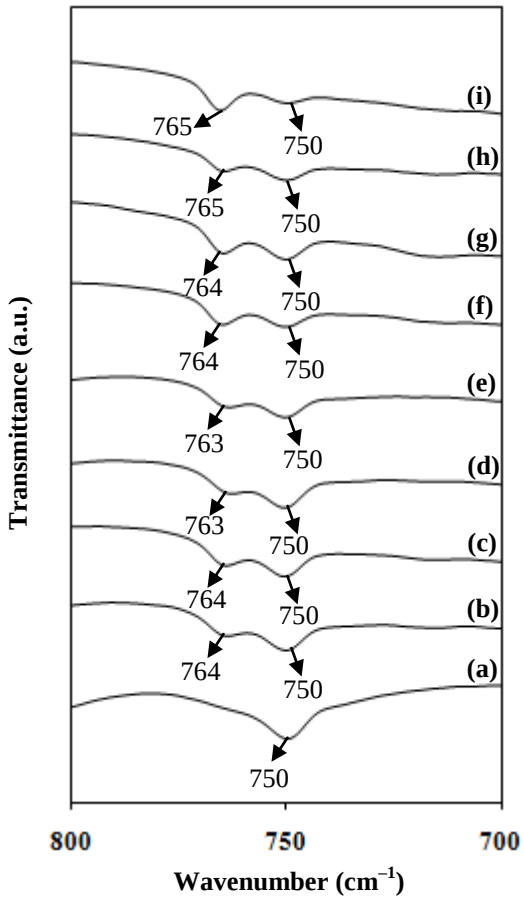

Figure 5.13 FTIR spectra in the region between 800 and 700 cm^{-1} of (a) MG0L, (b) MG5L, (c) MG10L, (d) MG15L, (e) MG20L, (f) MG25L, (g) MG30L, (h) MG35L and (i) MG40L

In pure MG30 sample, a band that peaks at 750 cm^{-1} (Figure 5.13 (a)) is attributable to the $\rho(C–H_2)$ rocking mode of PMMA grafted onto the NR. This band remained unchanged at 750 cm^{-1} in all the polymer–salt complexes. Upon the incorporation of lithium triflate, a band around 763–765 cm^{-1} appeared in all the $LiCF_3SO_3$–containing MG30 samples. This new band, $\delta(CF_3)$ originated from lithium triflate salt and was originally situated at 773 cm^{-1} as shown in Figure 5.2 (a). The presence of this new peak was also reported at ~772 cm^{-1} by Tan and Arof (2006) in hexanoyl chitosan–$LiCF_3SO_3$ films and at ~768 cm^{-1} by Ali *et al.* (2008) in MG30 polymer electrolytes. The large position shift of the band (8 to 10 cm^{-1}) to lower wavenumbers indicates that the environment of the triflate ion has changed which could be due to the coordination of Li^+ ions to the oxygen atoms of the carbonyl group and the $O–CH_3$ methoxy group.

5.3 Vibrational studies of MG30–$LICF_3SO_3$–$LiN(CF_3SO_2)_2$ films

Lithium imide was used to substitute lithium triflate in 70 wt. % MG30–30 wt. % $LiCF_3SO_3$ in order to study the effect of lithium imide on MG30–$LiCF_3SO_3$ samples by FTIR and EIS characterizations. Here, we will investigate the interactions between $LiCF_3SO_3$ and $LiN(CF_3SO_2)_2$ and the effect of different $LiCF_3SO_3$ and $LiN(CF_3SO_2)_2$ compositions on MG30 polymer electrolyte samples. Wavenumber shifts for the ν_a(S–N–S), $\nu_s(SO_2)$ and $\nu_a(CF_3)$ for the imide ion pairs with respect to free imide anion for polymer electrolytes have gained enormous interest in the past [Bakker *et al.*, 1995; Wang *et al.*, 1999; Wen *et al.*, 1996].

Figure 5.14 below shows the IR spectra of MG15L15I, MG20L10I and MG10L20I samples in the region 2000–600 cm^{-1}.

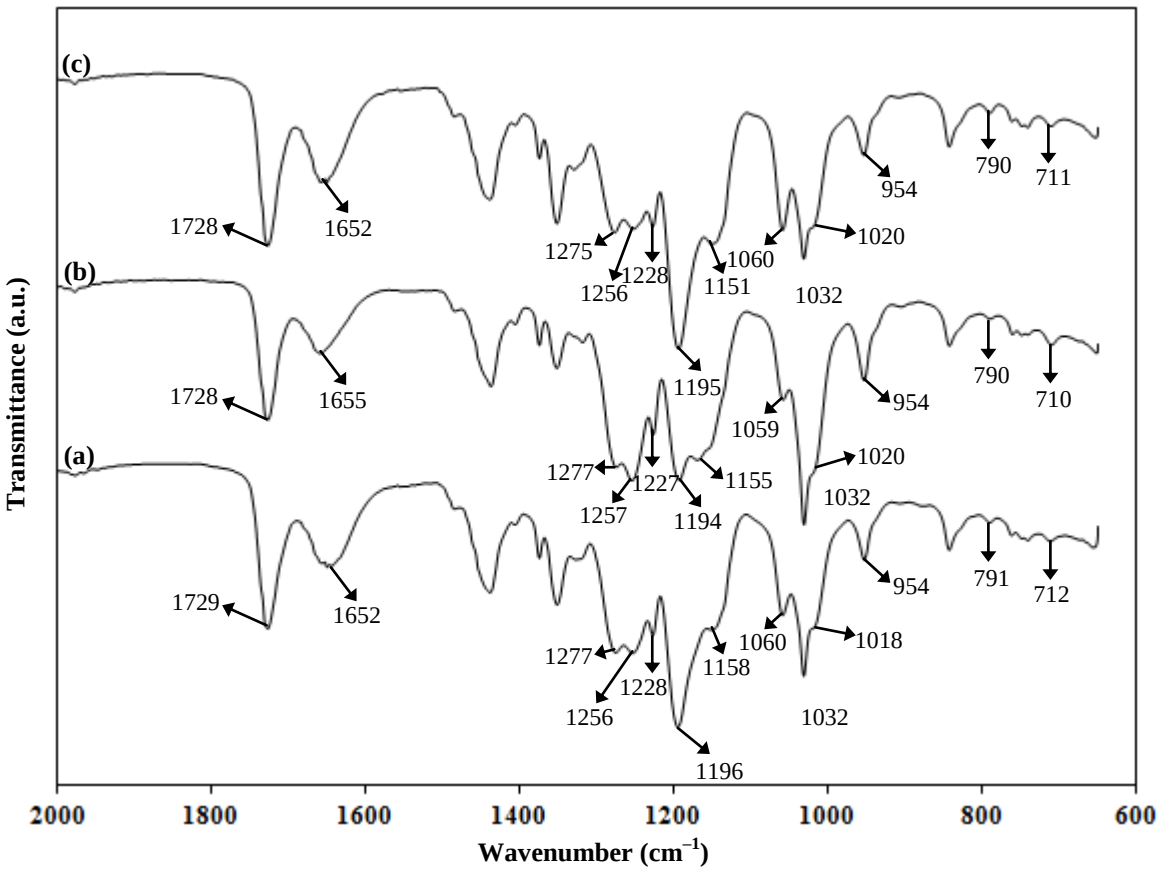

Figure 5.14 FTIR spectra in the region between 2000 and 650 cm^{-1} of (a) MG15L15I, (b) MG20L10I and (c) MG10L20I

The *v*(C=O) band of MG15L15I, MG20L10I and MG10L20I as shown in Figure 5.15 is observed at higher wavenumbers at 1729, 1728 and 1728 cm^{-1}, respectively, as compared to 1727 cm^{-1} in MG30L. Coordination of Li^+ onto the C=O group results in upshift of the *v*(C=O) band in the MG30–$LiCF_3SO_3$–$LiN(CF_3SO_2)_2$ polymer electrolytes.

Besides that, the band at 1648 cm^{-1} in MG30L shifted to 1652 cm^{-1} in both MG15L15I and MG10L20I samples, and to 1655 cm^{-1} in MG20L10I, which is close to the original position at 1663 cm^{-1} in pure MG30. The peak is also clearly observed, which indicate there is an interaction between the C=C and lithium salt.

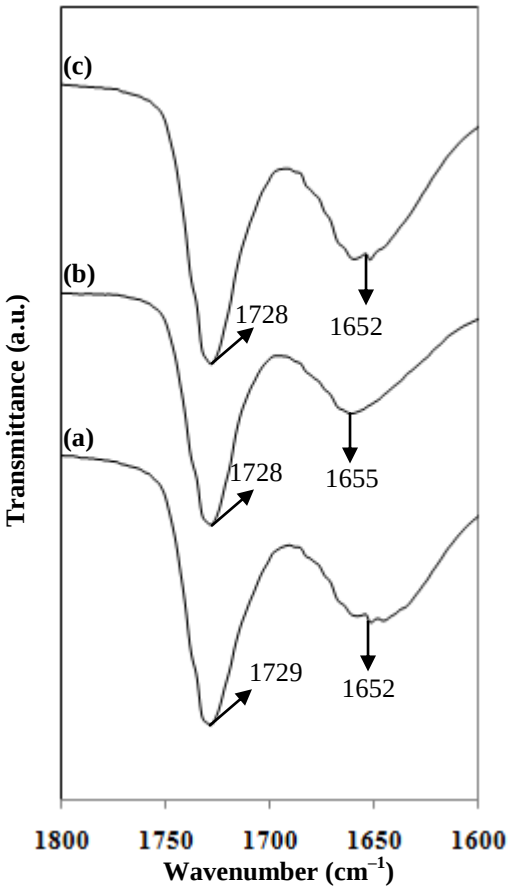

Figure 5.15 FTIR spectra in the region between 1800 and 1600 cm^{-1} of (a) MG15L15I, (b) MG20L10I and (c) MG10L20I

The deconvoluted bands from 1320 to 1200 cm^{-1} of varying composition of MG30–$LiCF_3SO_3$–$LiN(CF_3SO_2)_2$ samples are shown in Figure 5.16. The characteristic band of $LiCF_3SO_3$ present at 1292 cm^{-1} in the optimized single–salt sample, MG30L downshifted to 1286, 1285 and 1288 cm^{-1} in MG15L15I, MG20L10L and MG10L20I respectively. The $\nu_a(SO_3)$ band of lithium triflate at 1259 cm^{-1} in MG30L sample shifted to higher wavenumber at 1256 cm^{-1} in MG15L15I and MG10L20I and 1257 cm^{-1} in MG20L10I sample. The $\nu_s(CF_3)$ vibrational mode of $LiCF_3SO_3$ was observed to shift from 1231 cm^{-1} to lower wavenumbers at 1228 cm^{-1} in MG15L15I and MG10L20I. In MG20L10I, the $\nu_s(CF_3)$ band was found at 1227 cm^{-1}. The changes in wavenumbers of the three vibrational modes belonging to triflate anion indicate that addition of lithium imide into $LiCF_3SO_3$–containing MG30 samples has changed the environment of the triflate anion. This phenomenon implies that interaction has occurred between lithium

imide and the polymer. The $\tau(CH_2)$ band from MG30 which was present at 1247 cm^{-1} in MG30L shifted to 1244, 1245 and 1243 cm^{-1} in MG15L15I, MG20L10I and MG10L20I samples, respectively. The ν(C–O) of –COO– vibrational mode of PMMA grafted on MG30 previously found at 1279 cm^{-1} shifted to 1275 cm^{-1} in MG15L15I and to 1277 cm^{-1} in MG20L10I and MG10L20I samples. The higher wavenumber shift of ν(C–O) of –COO– band observed in MG15L15I (4 cm^{-1}) as compared to other double–salt containing MG30 samples indicates that interaction of Li^+ ions with the oxygen atom in C–O group of PMMA has occurred to a higher extent.

Figure 5.17 illustrates the IR vibrational modes between 1210 and 1110 cm^{-1} that are present in MG30L, MG15L15I, MG20L10I and MG10L20I samples. The $\delta_s(CH_2)$ in–plane bending mode of poly(isoprene) units which is present at 1196 cm^{-1} in the single–salt containing MG30L sample was found at 1194 to 1196 cm^{-1} in the double–salt MG30–$LiCF_3SO_3$–$LiN(CF_3SO_2)_2$ films. The $\nu_a(CF_3)$ band of lithium triflate in MG30L observed at 1177 cm^{-1} shifted to 1170 cm^{-1} in MG20L10I but this band disappeared in MG15L15I and MG10L20I samples. The band attributable to the $\tau(CH_2)$ twisting of PMMA at 1158 cm^{-1} in MG30L shifted to lower wavenumbers at 1151 to 1155 cm^{-1} in the double–salt containing MG30 polymer electrolytes. A new band located at 1136 cm^{-1} in all MG30 samples containing both lithium triflate and lithium imide salts at different compositions most probably belongs to $\nu_s(SO_2)$ band of lithium imide which was previously present at 1144 cm^{-1}. The downshift of the $\nu_s(SO_2)$ band shows that lithium imide has interacted with MG30.

Figure 5.18 shows the IR bands of single–salt MG30L and MG30 containing varying composition of lithium triflate and lithium imide between 1100 and 900 cm^{-1}.

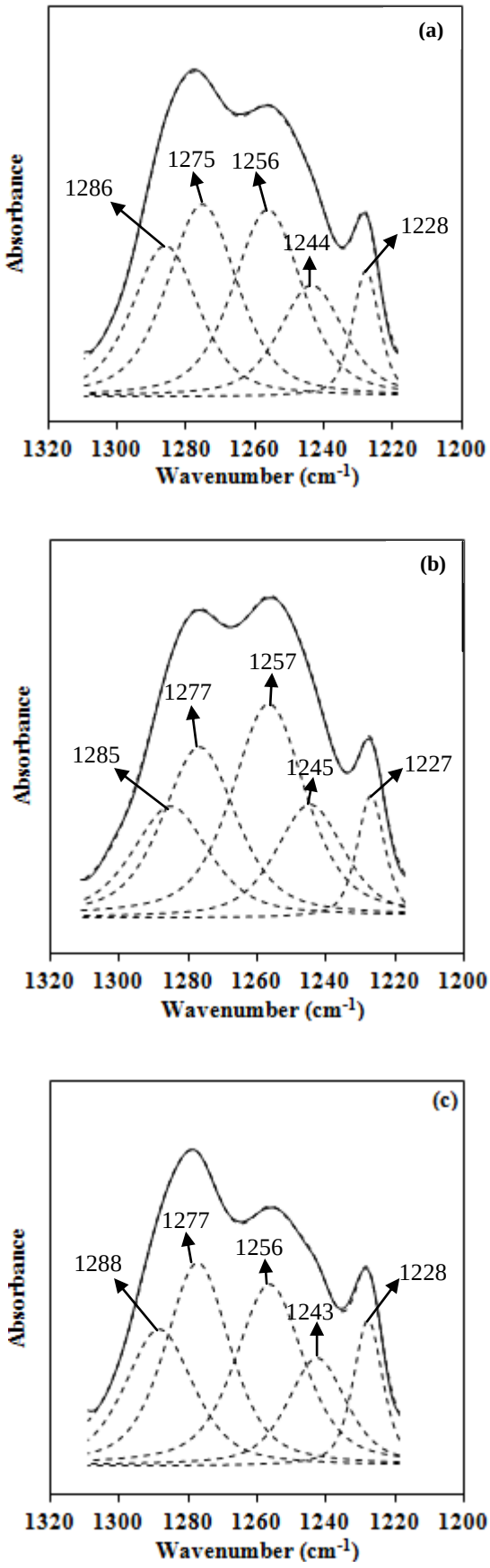

Figure 5.16 Deconvoluted FTIR spectra in the region between 1320 and 1200 cm^{-1} of (a) MG15L15I, (b) MG20L10I and (c) MG10L20I

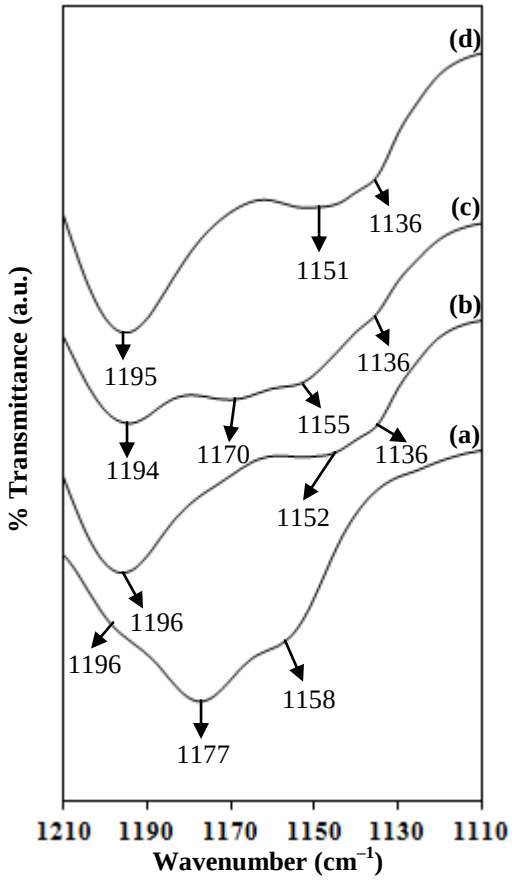

Figure 5.17 FTIR spectra in the region between 1210 and 1110 cm^{-1} of (a) MG30L, (b) MG15L15I, (c) MG20L10I and (d) MG10L20I

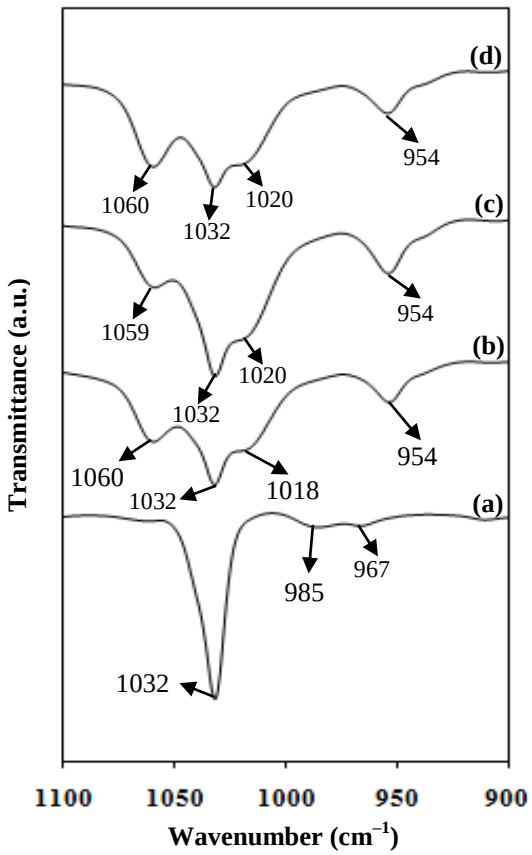

Figure 5.18 FTIR spectra in the region between 1100 and 900 cm^{-1} of (a) MG30L, (b) MG15L15I, (c) MG20L10I and (d) MG10L20I

In MG30L, the v_s(C–O–C) symmetric stretching of PMMA lies at 985 cm^{-1} while the $v_s(SO_3)$ band of lithium triflate is present at 1032 cm^{-1}. There is no change in the position of the $v_s(SO_3)$ band in the three samples as the band remained at 1032 cm^{-1}. Upon the addition of lithium imide salt into $LiCF_3SO_3$ added MG30 samples, three new peaks could be observed around 1060, 1020 and 954 cm^{-1} in the double–salt polymer electrolyte films. The peak observed at 1060 cm^{-1} in all the three samples is originated from v_a(S–N–S) mode of lithium imide salt. The band at 954 cm^{-1} is also present at the same position in MG15L15I, MG20L10I and MG10L20I samples. The v_s(C–O–C) symmetric stretching of PMMA have shifted from 985 cm^{-1} to between 1018 cm^{-1} and 1017 cm^{-1}. This show the lithium imide salt has a greater influence to this bonding.

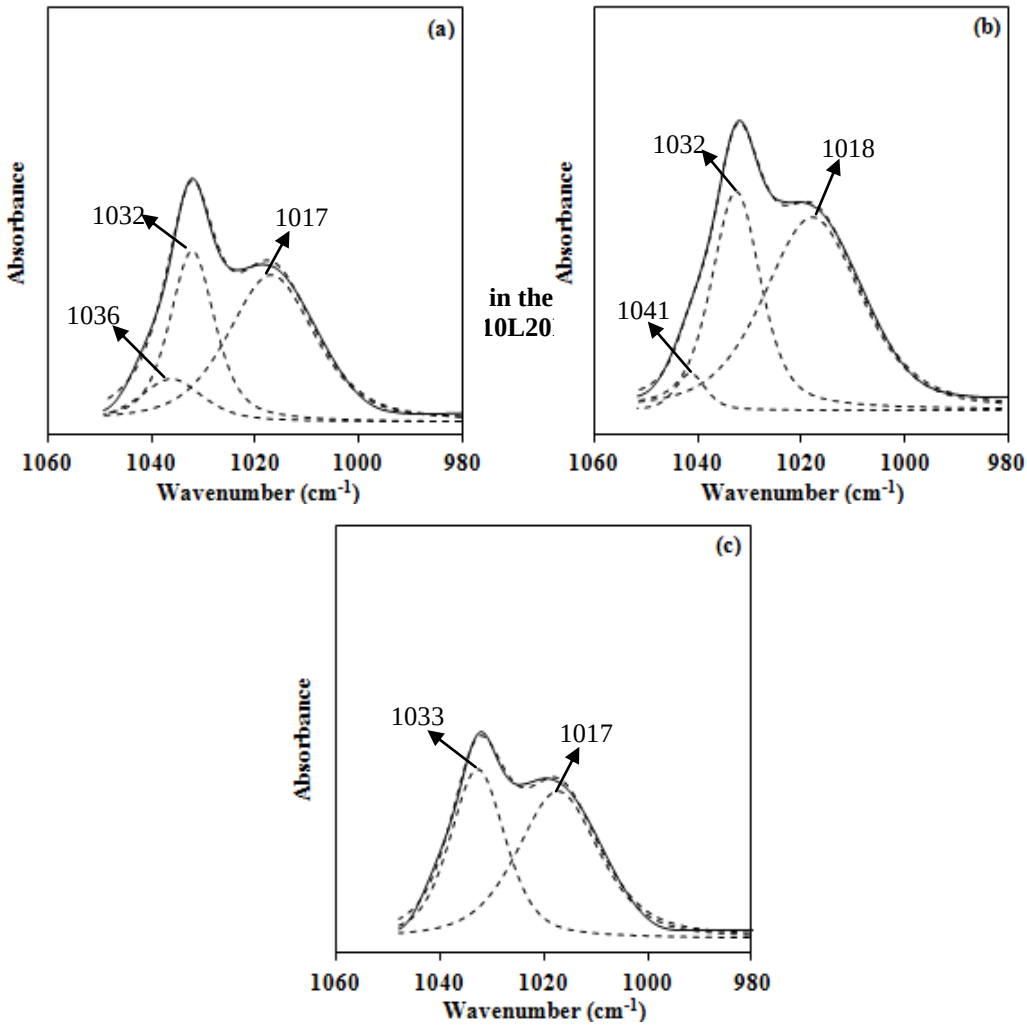

Figure 5.19 Deconvoluted FTIR spectra in the region between 1060 and 980 cm^{-1} of (a) MG20L10I, (b) MG10L20I and (c) MG15L15I

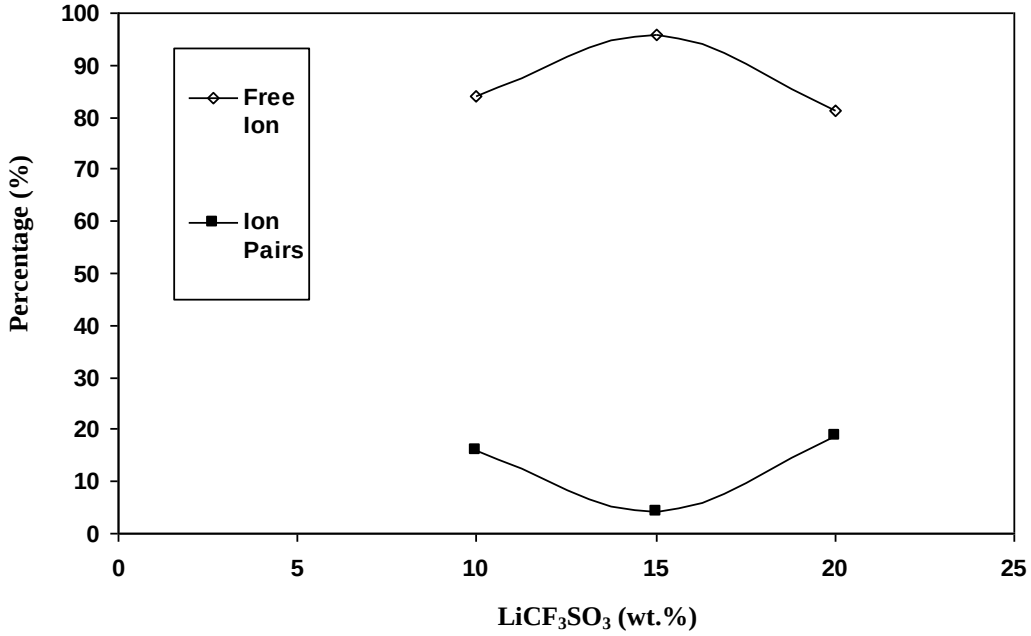

Figure 5.20 Variation of concentration of various states of ions in percentage (%) as a function of $LiCF_3SO_3$

It could be observed that in all samples, the intensity and area of free triflate ions were found to be noticeably larger than that of ion–pairs (Figure 5.19). It could be seen that MG15L15I contained the highest area of the free triflate ions and thus has the highest amount of free Li^+ ions that could contribute to conductivity. These results suggest that MG15L15I could be the most conducting film in the MG30–$LiCF_3SO_3$–$LiN(CF_3SO_2)_2$ polymer electrolyte system.

Figure 5.21 shows the vibrational modes of MG30, lithium triflate and lithium imide that are present in MG30L and MG30–$LiCF_3SO_3$–$LiN(CF_3SO_2)_2$ polymer electrolyte samples.

The presence of three bands in MG30L sample at 764, 750 and 714 cm^{-1} are attributable to $\delta(CF_3)$ mode of lithium triflate salt added into MG30, $\rho(C–H_2)$ of PMMA and an unassigned band of lithium triflate, respectively. An enlarged image of the IR spectrum of lithium triflate between 780 and 680 cm^{-1} is provided in Figure 5.22.

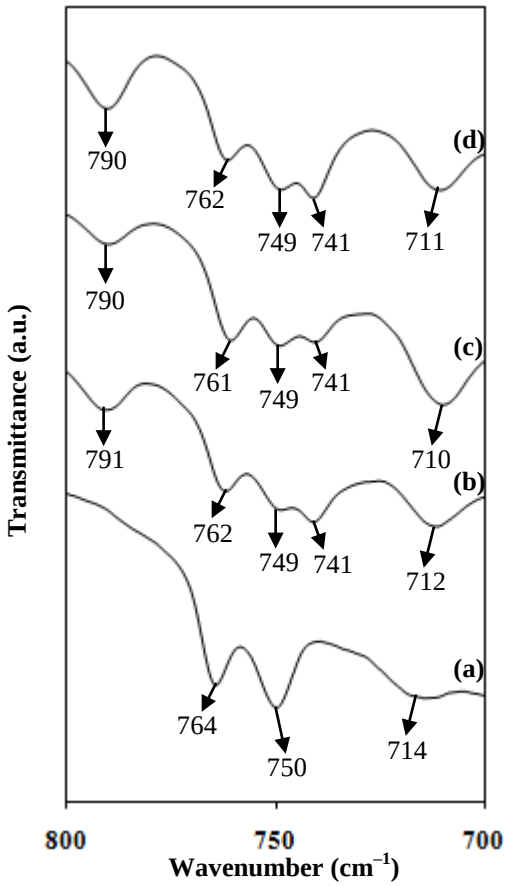

Figure 5.21 FTIR spectra in the region between 800 and 700 cm^{-1} of (a) MG30L, (b) MG15L15I, (c) MG20L10I and (d) MG10L20I

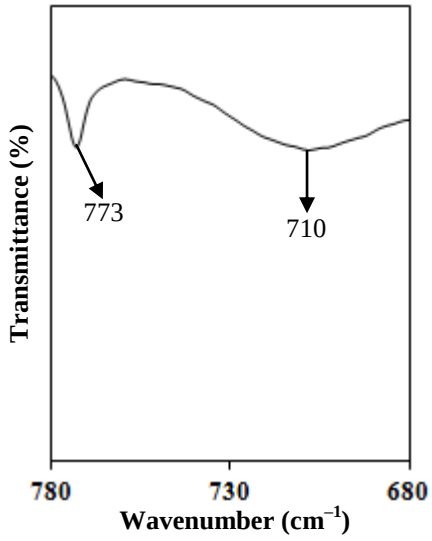

Figure 5.22 An enlarged IR spectrum of lithium triflate between 780 and 680 cm^{-1}

The band observed at 714 cm^{-1} is the result of the shifting from the original position at 710 cm^{-1} in the lithium triflate salt. After the addition of lithium imide salt, two new peaks could be observed. These two bands were located around 790 and 749 cm^{-1} which originated from *v*(C–S) combined with *v*(S–N), and *v*(S–N) modes, respectively. The two bands have shifted from their original wavenumbers at 799 and 747 cm^{-1} in pure lithium imide salt. According to Bakker *et al.* (1995) and Deepa *et al.*, (2004), the *v*(S–N) band located at ~750 cm^{-1} is due to ion–pairs, while free imide ion is located at ~739 cm^{-1}. Therefore, the shifting of the *v*(S–N) bands to lower wavenumbers in the samples containing double–salt indicates the tendency of free imide ions to be formed. This suggests that higher ionic conductivity values could be obtained when lithium imide is incorporated into the MG30–$LiCF_3SO_3$ samples.

5.4 Vibrational studies of MG30–$LiCF_3SO_3$–PEG200 films

FTIR spectra of PEG–plasticized polymer electrolytes have been reported by Shanmukaraj and Murugan (2005) and Rajendran *et al.* (2009). According to Rajendran *et al.* (2009), the rocking, C–O stretch, CH_2 twist, wagging and deformation vibrations of pure PEG with molecular weight 6000 g mol^{-1} were observed at IR wavenumbers 841, 986, 1282, 1343 and 1466 cm^{-1}, respectively. Shanmukaraj and Murugan reported the vibrational bands of PEG with molecular weight 4000 g mol^{-1} for C–O–C stretch, *v*(C–O–C) and CH_2 rocking at 1111 and 950 cm^{-1}, respectively. Vibrational modes of OH stretch, *v*(OH) and symmetrical stretch, $v_s(CH_2)$ of PEG–400 were observed at 3448 and 2866 cm^{-1} by Ozturk *et al.* (2009). For our work, PEG with molecular weight 200 g mol^{-1} was used and its IR spectrum is shown in Figure 5.23. The assignments of IR vibrations are listed on Table 5.3.

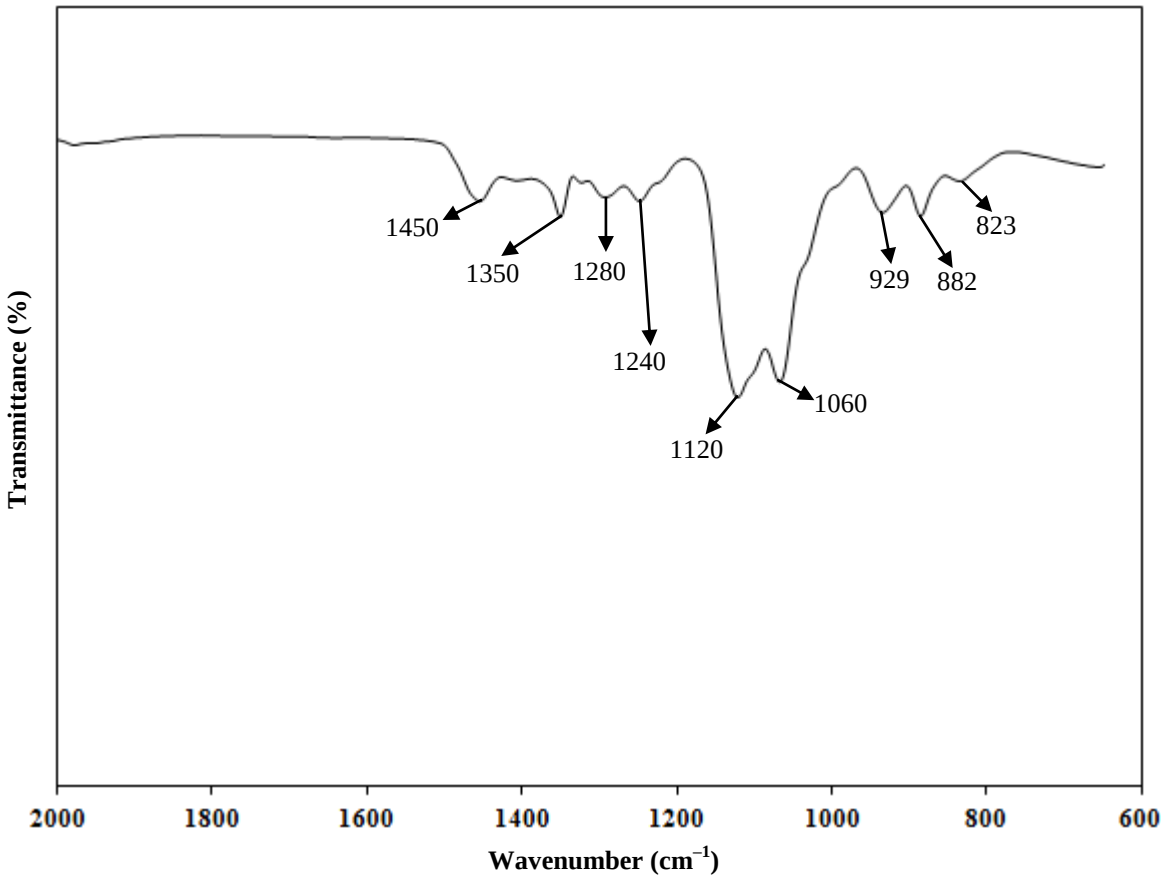

Figure 5.23 FTIR spectrum of PEG200

Table 5.3: Vibrational assignments of PEG200

Wavenumber (cm^{-1})	Assignment
3410	ν(OH)
2860	$\nu_s(CH_2)$
1450	CH_2 deformation
1350	CH_2 wagging
1280	CH_2 twisting
1120	ν(C–O–C)
929	CH_2 rocking
823	Rocking vibration of PEG

Figure 5.24 depicts the IR spectrum of PEG plasticized 70 wt. % MG30–30 wt. % $LiCF_3SO_3$ samples.

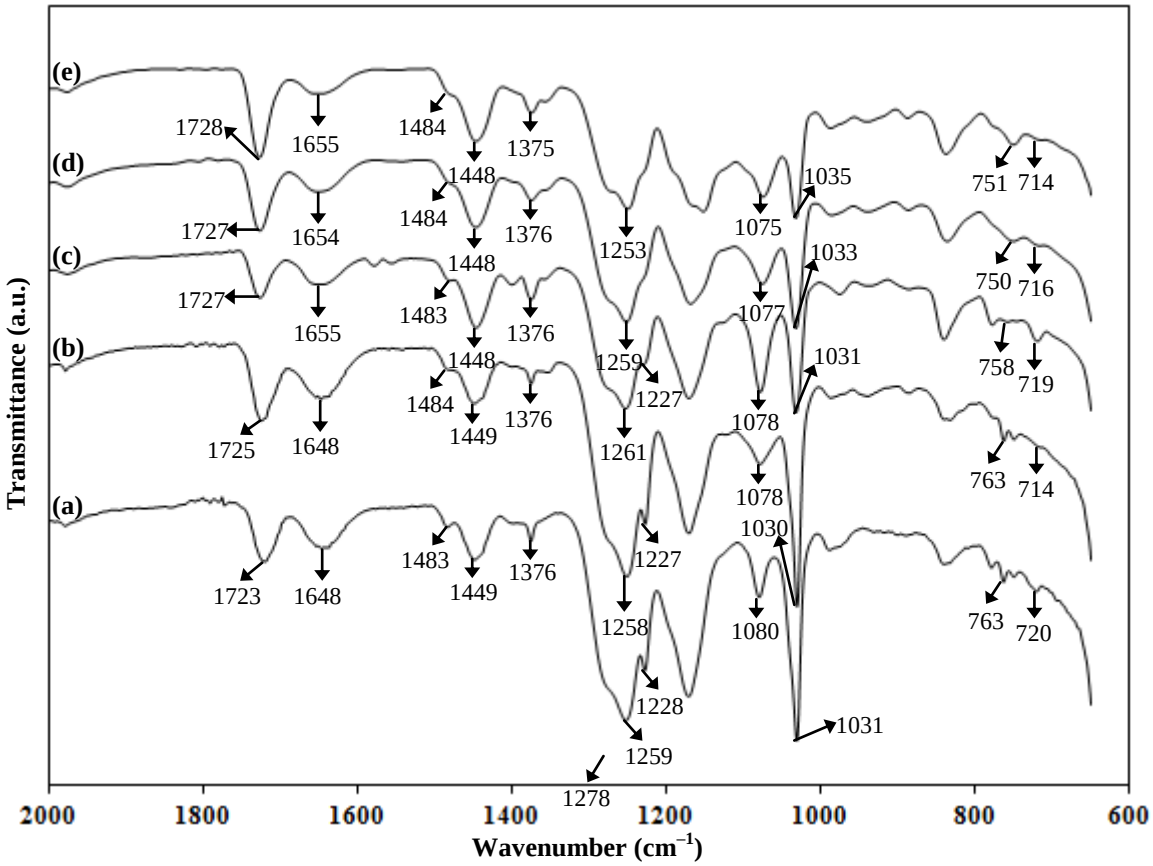

Figure 5.24 FTIR spectra in the region between 2000 and 650 cm^{-1} of (a) MG30L–5P, (b) MG30L–7P, (c) MG30L–10P, (d) MG30L–20P and (e) MG30L–30P

Figure 5.24 illustrates the FTIR spectra for 70 wt. % MG30–30 wt. % $LiCF_3SO_3$ added with various amounts of PEG in the region of 1600 cm^{-1} to 1800 cm^{-1}. In MG30L sample, the *v*(C=O) band was found at 1727 cm^{-1} while the peak due to overlap of *v*(C=C) stretching mode of natural rubber and characteristic peak of lithium triflate salt was located at 1648 cm^{-1}. Upon the incorporation of PEG200 as plasticizer, the *v*(C=O) band was slightly downshifted to 1723 cm^{-1} in MG30L–5P. With addition of higher amounts of PEG200, this band shifted to higher wavenumbers at 1725 cm^{-1} in MG30–7P, 1727 cm^{-1} in both MG30–10P and MG30–20P and lastly, 1728 cm^{-1} in MG30–30P sample.

The higher wavenumber of the *v*(C=O) band in most of the plasticized polymer electrolytes indicate weaker coordination of Li^+ ions onto the oxygen of the carbonyl

group possibly caused by the interaction of PEG with MG30. Upshift of the C=O band was also observed in the MG30–$LiCF_3SO_3$–$LiN(CF_3SO_2)_2$ polymer electrolytes. Since Li^+ ions are more weakly coordinated to the carbonyl group, the cations are more labile and therefore can be transported more easily from one coordinating site to another, hence the plasticization of MG30 should produce higher ionic conductivity.

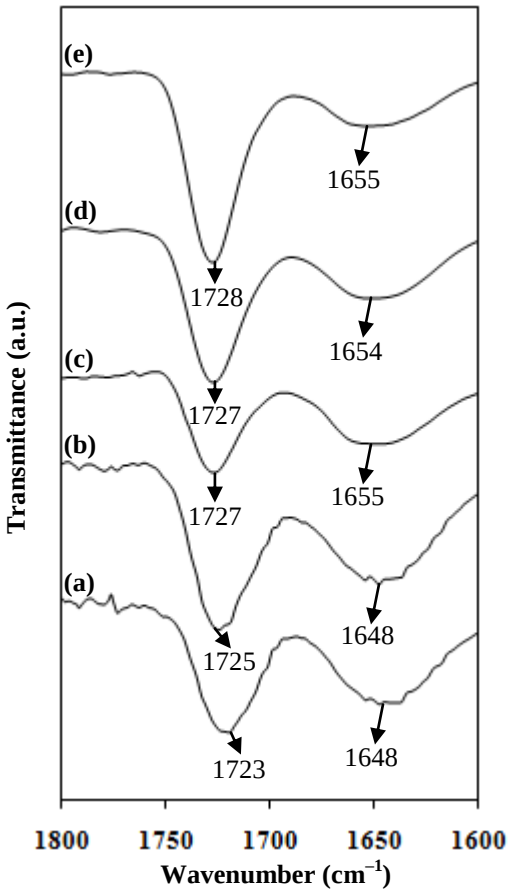

Figure 5.25 FTIR spectra in the region between 1800 and 1600 cm^{-1} of (a) MG30L–5P, (b) MG30L–7P, (c) MG30L–10P, (d) MG30L–20P and (e) MG30L–30P

The band located at 1648 cm^{-1} maintained its position into MG30–5P and MG30–7P and moved to higher wavenumbers at 1655, 1654 and 1655 cm^{-1} in MG30–10P, MG30–20P and MG30–30P samples, respectively. The large shift of 6 to 7 cm^{-1} of this band in MG30–$LiCF_3SO_3$ samples containing 10 wt.% PEG and above suggests that there could be more Li^+ free ions that could contribute towards conductivity. Figure 5.25 illustrates deconvolution of the bands between 1800 and 1600 cm^{-1}.

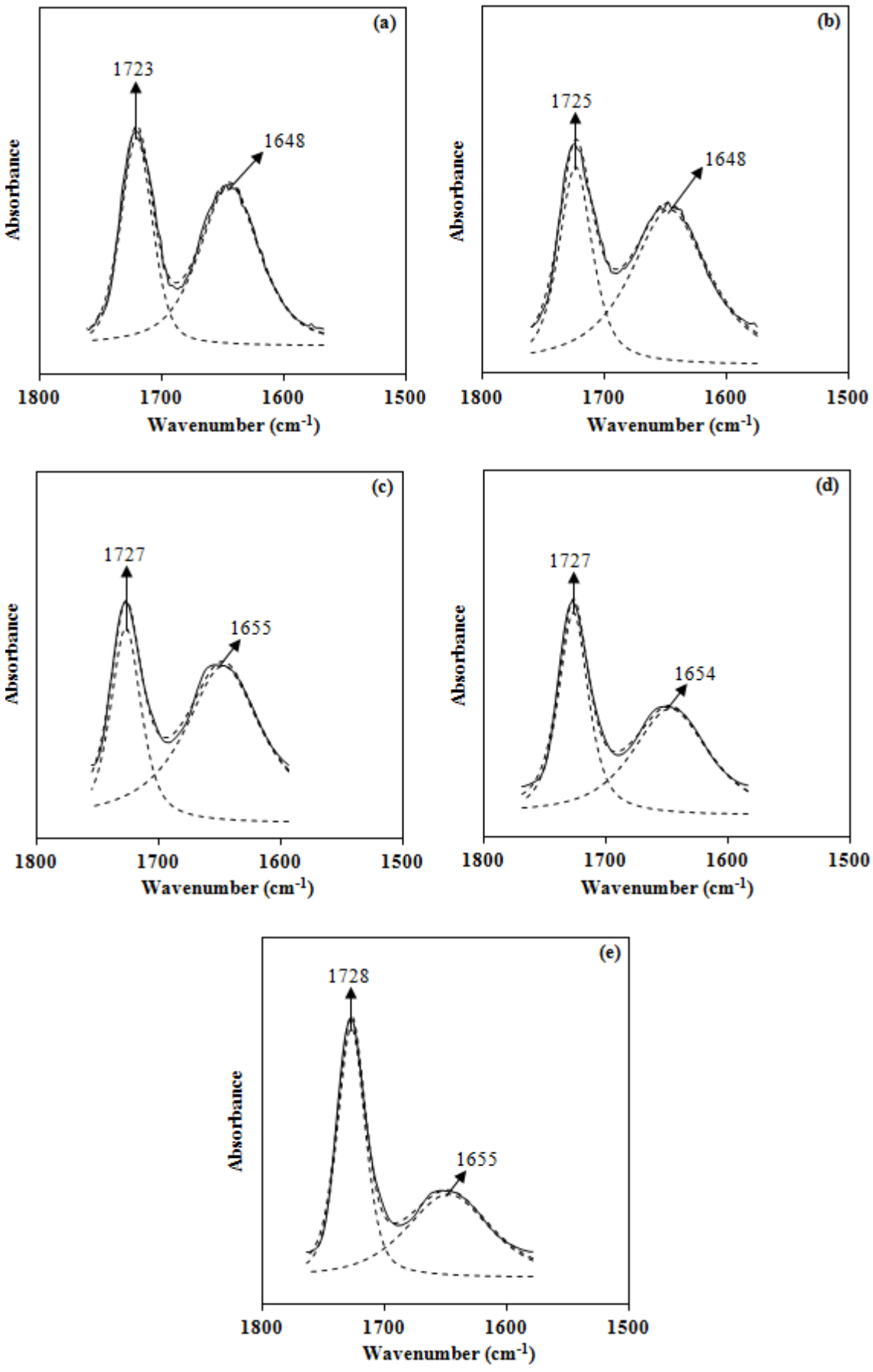

Figure 5.26 Deconvoluted FTIR spectra in the region between 1800 and 1500 cm^{-1} of (a) MG30L–5P, (b) MG30L–7P, (c) MG30L–10P, (d) MG30L–20P and (e) MG30L–30P

Figure 5.27 shows the wavenumber region between 1550 and 1350 cm^{-1} for the MG30L and PEG–plasticized MG30 polymer electrolytes.

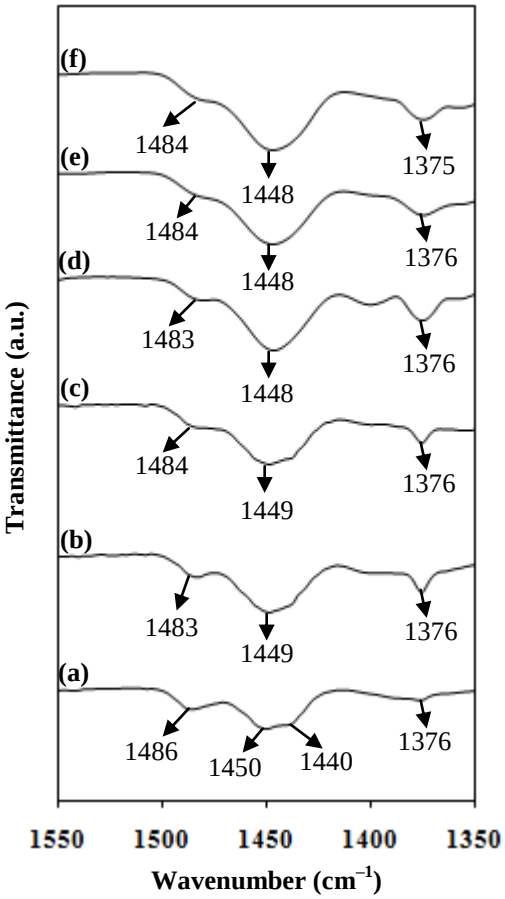

Figure 5.27 FTIR spectra in the region between 1550 and 1350 cm^{-1} of (a) MG30L, (b) MG30L–5P, (c) MG30L–7P, (d) MG30L–10P, (e) MG30L–20P and (f) MG30L–30P

The $\beta(CH_3)$ vibrational mode of polyisoprene did not exhibit distinct changes in the spectrum of PEG–plasticized samples. Upon addition of PEG, asymmetric bending of CH bond in $–C–CH_3–$ of PMMA in MG30 shifted from 1486 cm^{-1} to 1483 cm^{-1} in MG30L–5P and MG30L–10P and to 1484 cm^{-1} in MG30L–7P, MG30L–20P and MG30L–30P. Several bands belonging to the polymer host, MG30 and the plasticizer, PEG overlapped with each other in the region around 1500 to 1420 cm^{-1}. In order to separate overlapping bands, the deconvoluted IR spectra of the MG30 films containing various wt. % PEG between 1520 and 1400 cm^{-1} are shown in Figure 5.28.

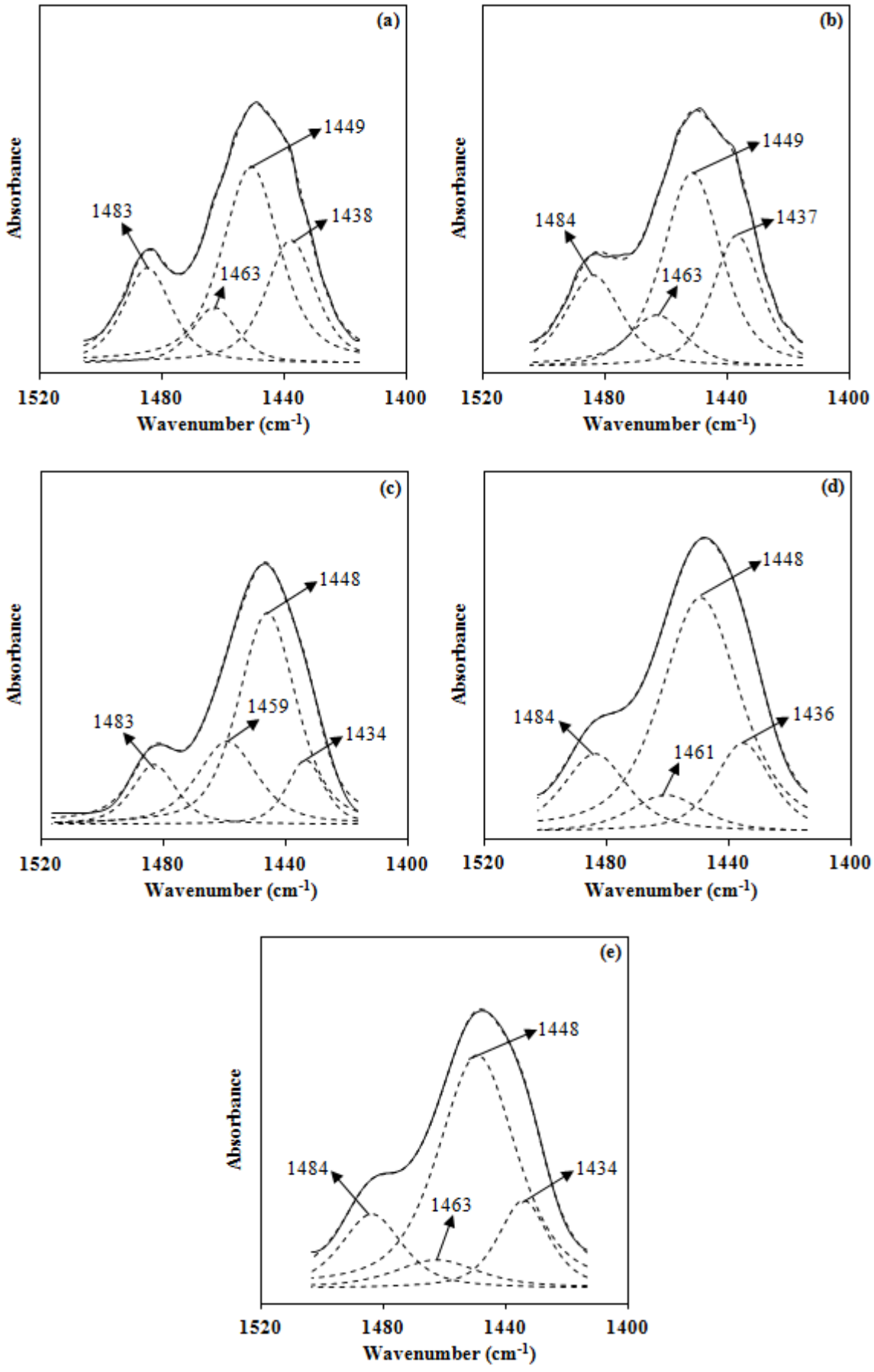

Figure 5.28 Deconvoluted FTIR spectra in the region between 1520 and 1400 cm^{-1} of (a) MG30L–5P, (b) MG30L–7P, (c) MG30L–10P, (d) MG30L–20P and (e) MG30L–30P

From Figure 5.28, it can be observed that the CH_2 deformation band of PEG was present in the plasticized MG30 electrolytes in the region between 1459 and 1463 cm^{-1}. Among all samples, MG30L–10P displays the most intense band at 1459 cm^{-1} (Figure 5.28 (c)) which implies that the amount of PEG interacting with MG30 is highest in the sample. Other vibrational mode includes the CH_2 scissoring vibrational modes of PMMA located at 1434 to 1438 cm^{-1}.

Figure 5.29 depicts the IR spectra between 1350 and 1210 cm^{-1} for MG30L and the PEG–plasticized polymer electrolyte films. It can be observed that band envelopes exist where several bands overlapped with each other. The IR envelopes were deconvoluted as shown in Figure 5.30 in order to distinguish between individual IR bands. The characteristic band of $LiCF_3SO_3$ present shifted slightly from 1292 cm^{-1} in MG30L to 1290 to 1294 cm^{-1} in the PEG–plasticized MG30 samples. The $\nu_a(SO_3)$ band of the salt at 1259 cm^{-1} also shifted to wavenumber at 1258 to 1261 cm^{-1} in the polymer–salt–plasticizer system.

The $\nu_s(CF_3)$ vibrational mode of $LiCF_3SO_3$ did not show distinct changes in its position from 1228 cm^{-1} in the unplasticized MG30L sample and were observed at 1227 and/or 1228 cm^{-1} in all the PEG–containing MG30 films. The $\tau(CH_2)$ band from MG30 which was present at 1247 cm^{-1} in MG30L could be observed at 1243 to 1249 cm^{-1} in the MG30–$LiCF_3SO_3$ samples added with PEG. The ν(C–O) of –COO– vibrational mode before the incorporation of PEG as plasticizer was present at 1279 cm^{-1} in MG30L sample, and did not show any change in the position.

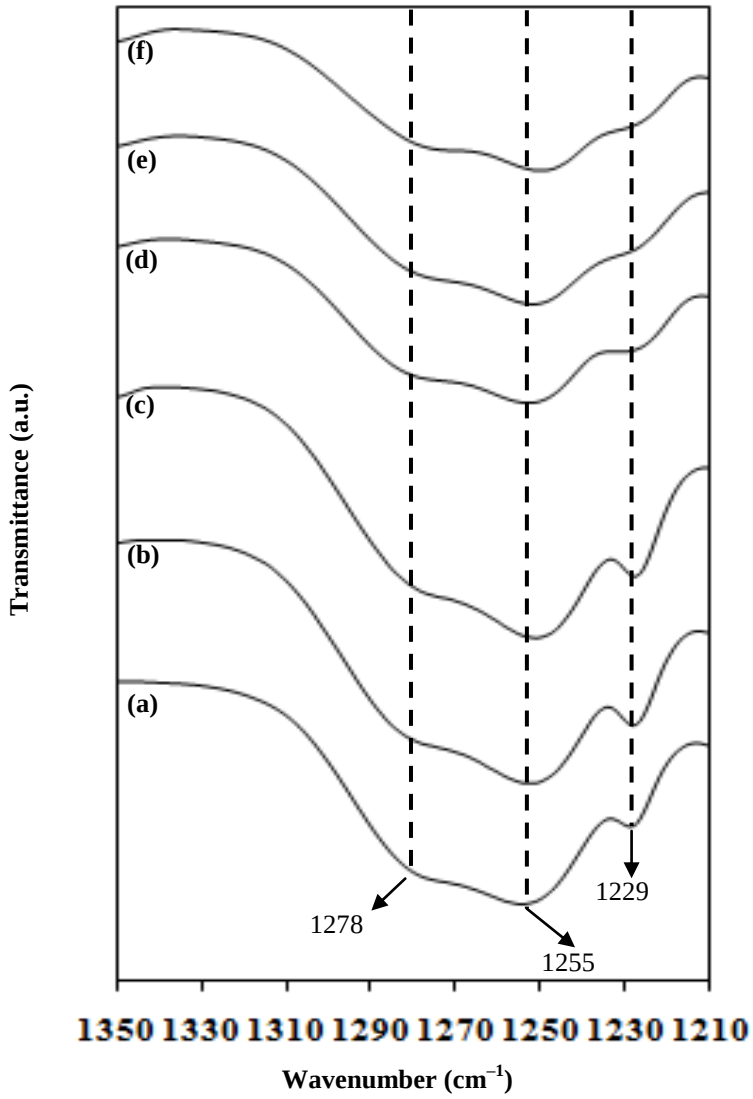

Figure 5.29 FTIR spectra in the region between 1350 and 1210 cm^{-1} of (a) MG30L, (b) MG30L–5P, (c) MG30L–7P, (d) MG30L–10P, (e) MG30L–20P and (f) MG30L–30P

Figure 5.31 depicts the IR spectra of MG30L and PEG–plasticized MG30 samples in the wavenumber range from 1100 to 1000 cm^{-1}.

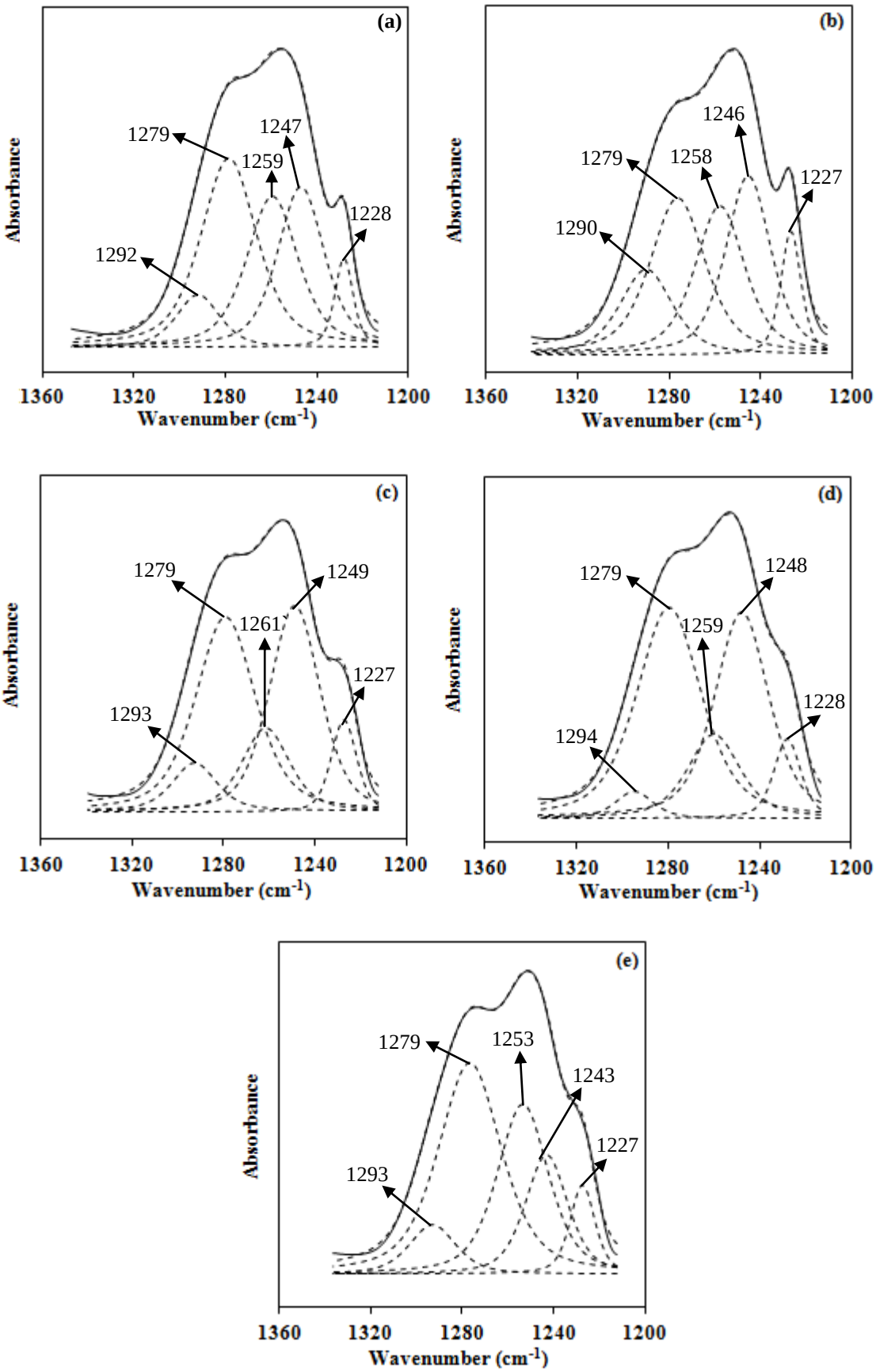

Figure 5.30 FTIR spectra in the region between 1360 and 1200 cm^{-1} of (a) MG30L–5P, (b) MG30L–7P, (c) MG30L–10P, (d) MG30L–20P and (e) MG30L–30P

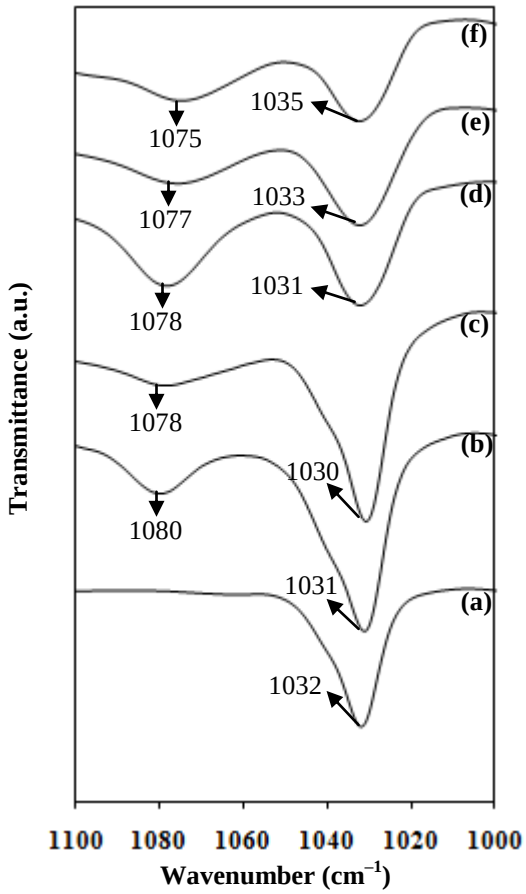

Figure 5.31 FTIR spectra in the region between 1100 and 1000 cm^{-1} of (a) MG30L, (b) MG30L–5P, (c) MG30L–7P, (d) MG30L–10P, (e) MG30L–20P and (f) MG30L–30P

Upon the addition of PEG200 into MG30–$LiCF_3SO_3$, a new peak around 1080 to 1075 cm^{-1} was observed in the PEG plasticized samples. This band originates from the characteristic band of PEG which is located at 1060 cm^{-1} in the pure sample (Figure 5.21). As can be observed in Figure 5.31 shown above, the $\nu_s(SO_3)$ band of lithium triflate salt shifted from 1032 to 1031 cm^{-1} in all the plasticized samples. The shift of this band to lower wavenumbers could suggest the increase in the number of free ions. In order to determine the fraction of free ions, ion pairs and ion aggregates in the plasticized samples, deconvolution of IR bands in the region between 1070 and 1000 cm^{-1} was conducted, and is shown in Figure 5.32.

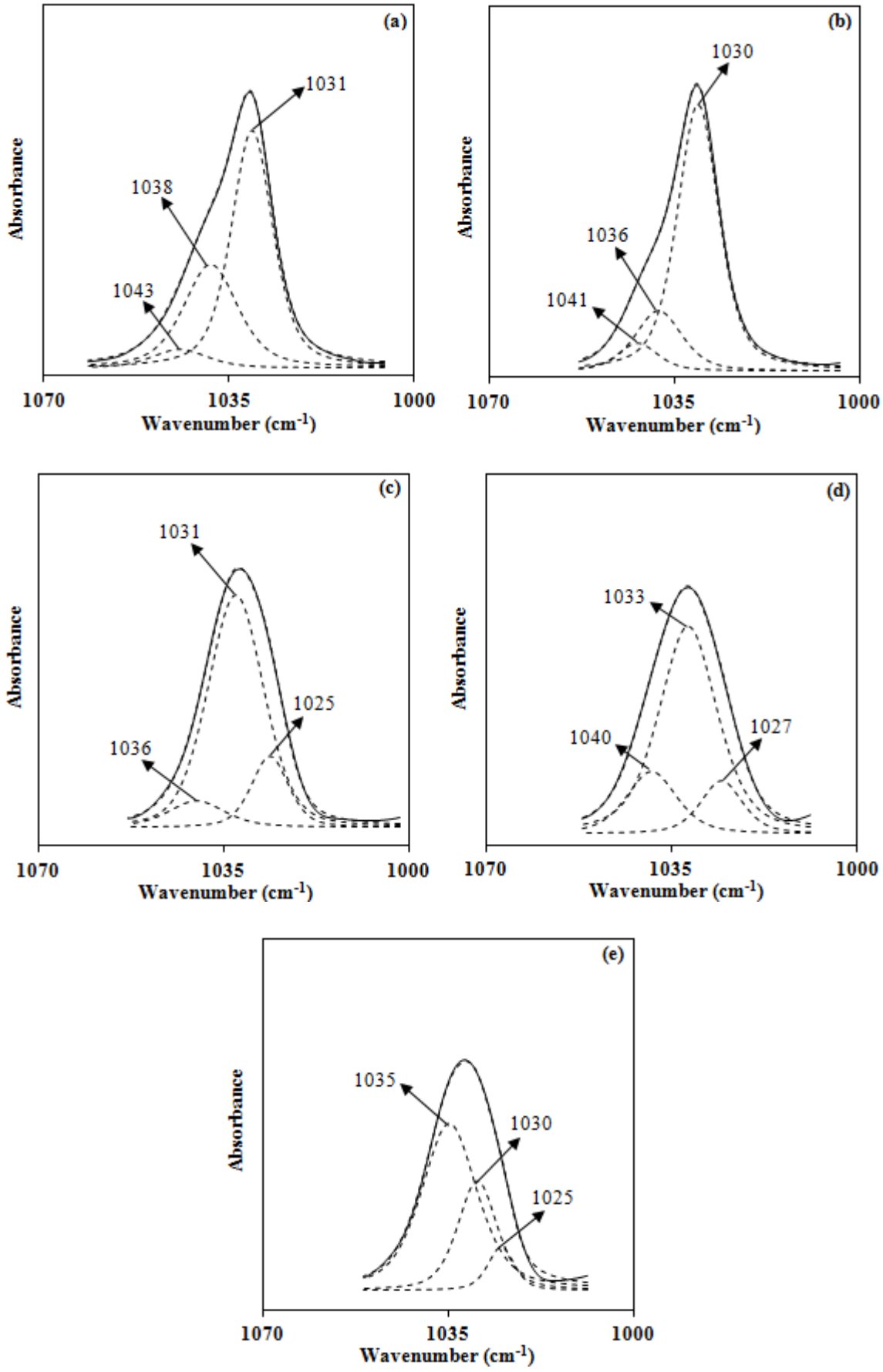

Figure 5.32 Deconvoluted FTIR spectra in the region between 1070 and 1000 cm^{-1} of (a) MG30L–5P, (b) MG30L–7P, (c) MG30L–10P, (d) MG30L–20P and (e) MG30L–30P

As mentioned earlier, the IR bands located between 1050 and 1000 cm^{-1} come from the different types of the $v_s(SO_3)$ band (Bernson and Lindgren, 1995). In MG30–$LiCF_3SO_3$ sample containing 5 wt. % of PEG200, the IR spectra show the presence of three bands which could be attributable for ion pairs (1043 and 1038 cm^{-1}) and free ions (1031 cm^{-1}) of the triflate salt, respectively. When added with more PEG200 in MG30–7P sample, these bands shifted slightly to lower wavenumbers to 1041, 1036 and 1030 cm^{-1}. When added with 10 wt.% and above of the plasticizer, these bands experienced larger shifts to 1036, 1031 and 1025 cm^{-1} in MG30–10P, 1040, 1033 and 1027 cm^{-1} in MG30–20P and 1035, 1030 and 1025 cm^{-1} in MG30–30P. As lower wavenumbers of this band promotes the presence of free triflate ions, the shift of the three bands to lower wavenumbers in MG30–10P, MG30–20P and MG30–30P indicates higher amounts of free ions in the latter samples. However, these bands in MG30–20P are at higher wavenumbers as compared to MG30–10P, and the fraction of ion pairs in MG30–30P is the highest among the three bands. The plots of area fraction in percentage (%) for free ions and ion pairs versus PEG content is shown in Figure 5.33.

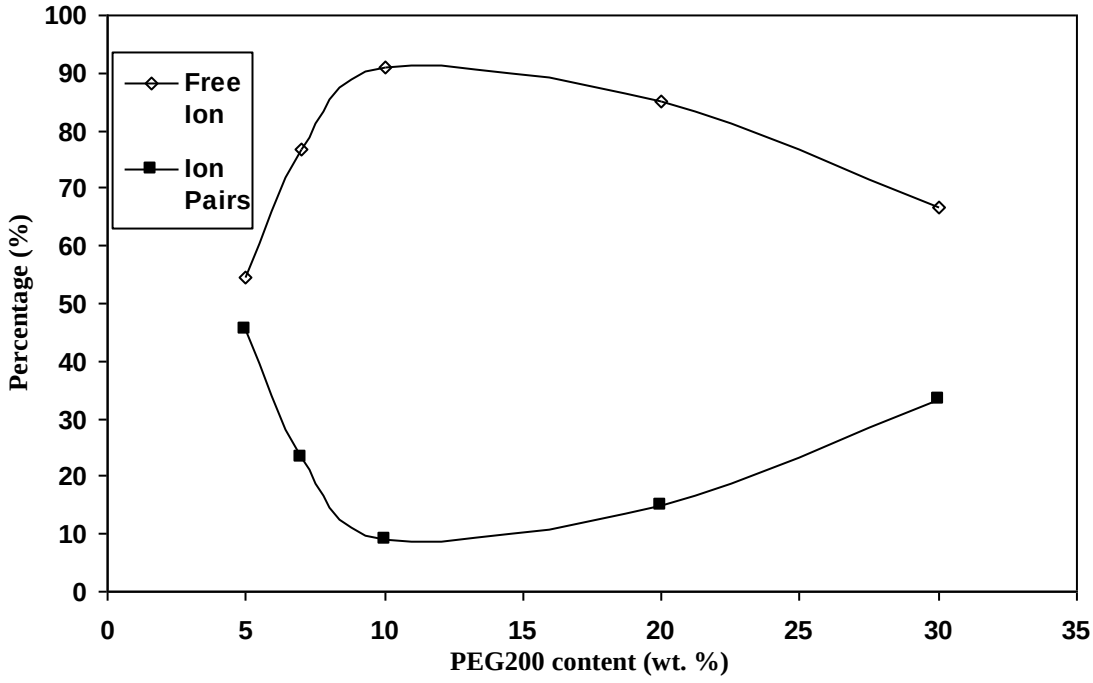

Figure 5.33 Variation of concentration of various states of ions as a function of PEG content

It can be observed from Figure 5.33 that MG30L–10P has the highest amount of free ions. Therefore, this could indicate that the sample containing 10 wt. % PEG200 which is MG30–10P could exhibit the highest ionic conductivity.

The vibrational modes belonging to MG30, lithium triflate and PEG within the wavenumber range between 800 and 700 cm^{-1} are shown in Figure 5.34. Before the incorporation of PEG into the optimized MG30–$LiCF_3SO_3$ composition, the $\rho(C–H_2)$ rocking mode of PMMA grafted onto the NR located at 750 cm^{-1}, $\delta(CF_3)$ of the lithium triflate salt at 764 cm^{-1} and the characteristic band of the salt at 714 cm^{-1} were present in MG30L sample.

The $\rho(C–H_2)$ rocking mode did not significantly shift in the spectrum of plasticized MG30 samples added with 5, 7, 20 and 30 wt. % PEG. In MG30L–10P sample, the $\rho(C–H_2)$ rocking mode of MG30 was found at lower wavenumber at 746 cm^{-1}. This phenomenon indicates that larger interaction has occurred between PEG and MG30 in MG30L–10P sample as compared to other plasticized MG30 films. The $\delta(CF_3)$ of lithium triflate at 764 cm^{-1} downshifted slightly to 763 cm^{-1} in the presence of 5 and 7 wt.% PEG. In MG30L–10P, the $\delta(CF_3)$ decreased in intensity and downshift to a larger extent to 758 cm^{-1}. The existence of the $\delta(CF_3)$ band at much lower wavenumber (758 cm^{-1}) in MG30L–10P indicates much weaker interaction between Li^+ cations and $CF_3SO_3^-$ anions and thus, the tendency to form free triflate ions is highest in the sample. Besides that, MG30L–10P also exhibits the largest lithium triflate band at 719 cm^{-1} which may indicate larger amount of triflate anions in the sample as shown in Figure 5.34 (d).

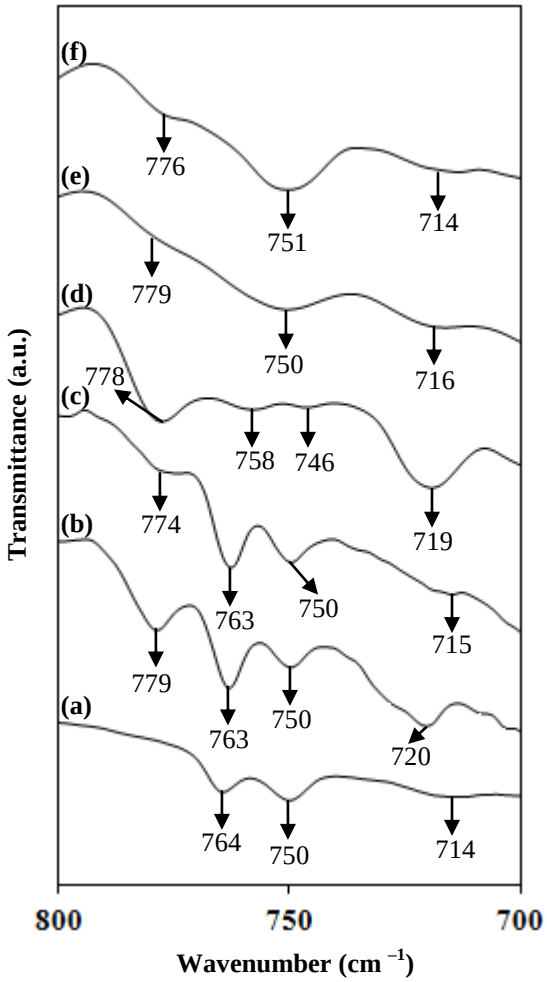

Figure 5.34 Deconvoluted FTIR spectra in the region between 800 and 700 cm^{-1} of (a) MG30L (b) MG30L–5P, (c) MG30L–7P, (d) MG30L–10P, (e) MG30L–20P and (f) MG30L–30P

In samples containing higher PEG contents, this band diminished and could not be observed in MG30L–20P and MG30L–30P samples. The disappearance of the $\delta(CF_3)$ band of lithium triflate as observed in MG30L–20P and MG30L–30P films indicate the decrease in the amount of free triflate anions at high content of PEG. Thus, it is expected that coordination of Li^+ ions coordinate the most to MG30L–10P sample and reduces at higher PEG contents above 10 wt.%.

5.5 Summary

From FTIR studies, both lithium salt, $LiCF_3SO_3$ and $LiN(CF_3SO_2)_2$ has interacted with MG30 at the carbonyl (C=O) function group, C=C bond and –O–CH_3– methoxy group since the bands have shifted indicating complexation has occurred.